Progress in Mid-IR Lasers Based on Cr and Fe-Doped II–VI Chalcogenides

Sergey B. Mirov, Vladimir V. Fedorov, Dmitry Martyshkin, Igor S. Moskalev, Mike Mirov, and Sergey Vasilyev

(Invited Paper)

***Abstract*—Transition metal (TM) doped II–VI chalcogenide laser materials offer a unique blend of physical, spectroscopic, and technological parameters that make them the gain media of choice for cost effective broadly tunable lasing in the Mid-IR. The II–VI semiconductor hosts provide a low phonon cut-off, broad IR transparency, and high thermal conductivity. When doped with transition metal ions, these materials feature ultrabroadband gain, low saturation intensities, and large pump absorption coefficients. This combined with the low-cost mass production technology of crystal fabrication by postgrowth thermal diffusion, as well as broad availability of convenient pump sources, make these materials ideal candidates for broadly tunable mid-IR lasing in CW, gain-switched, free running, and mode-locked regimes of operation. This review summarizes experimental results on optically pumped lasers based on Cr and Fe doped II–VI wide band semiconductors providing access to the 1.9–6 μm spectral range with a high (exceeding 60%) efficiency, multi-Watt-level (18 W in gain switch and 30 W in pure CW) output powers, tunability in excess of 1000 nm, short-pulse ($<$50 fs) multi-watt oscillation, multi-Joule long-pulse output energy, and narrow spectral linewidth ($<$100 kHz).**

***Index Terms*—Laser, mid-infrared, tunable, transition metal, wide-band semiconductor.**

I. Introduction

MIDDLE-infrared (mid-IR) laser sources are in great demand for a variety of applications including molecular spectroscopy; multi-photon microscopy; remote sensing for environmental monitoring, industrial process control, and medical diagnostics; material processing of polymers, glass and composites; free space communication; oil and gas prospecting; surgical, dental and cosmetology procedures; as well as numerous defense related applications. Mid-IR wavelengths are currently addressed by nonlinear optical conversion techniques, lead-salt diode lasers, antimonide lasers, quantum cascade semiconductor lasers, rare-earth doped crystalline lasers, as well as transition metal (TM) doped II-VI semiconductor (chalcogenide) lasers. The latter in particular, have recently come of age and are arguably the lasers of choice for cost-effective broadly tunable mid-IR lasing.

TM^{2+} doped wide bandgap II-VI semiconductor crystals were first introduced to the scientific community as effective mid-IR gain media by scientists from the Lawrence Livermore National Laboratory (LLNL) [1], [2]. The heavy ions in the II-VI crystals provide a low energy optical phonon cut-off, decreasing the efficiency of impurity non-radiative decay. II-VI semiconductors crystallize as tetrahedrally coordinated structures enabling small crystal field splitting that places the TM impurity transitions in the mid-IR spectral range. Overall, TM doped II-VI chalcogenides feature favorable spectroscopic characteristics necessary for efficient mid-IR lasing. Among them—a four-level energy structure, an absence of excited state absorption, broad absorption bands overlapping with many convenient fiber laser sources, a broad vibronic emission band enabling wide tunability, and (for Cr doped II-VI media) high—close to 100% quantum efficiency of fluorescence at room temperature (RT).

After these pioneering publications, the major attention was focused on Cr:ZnSe crystals having among other TM:II-VI compounds one of the most favorable combinations of thermal, optical, and spectroscopic properties. Initial progress in Cr:ZnSe lasers included: direct diode excitation [3]–[5]; continuous wave (CW) lasing with efficiency exceeding 60% [6]; gain switched lasing with 18.5 W average power [7]; the range of tunability over 1880–3100 nm [8]; first microchip [9], [10] and disk laser [11] operations; single-frequency operation with linewidth up to 100 kHz [12]–[14]; random lasing [15]–[17]; multi-line and ultra-broadband operation in spatially dispersive cavities [18]; lasing via photo-ionization transitions [19], and gain-switched (2 mJ) as well as CW (250 mW) operations of the Cr:ZnSe hot-pressed ceramic [20], [13].

Broad emission bands of TM:II-VI materials offer unique opportunities for generation of mid-IR ultra-short laser pulses. All significant milestones in the development of mode-locked TM:II-VI lasers were at first reached with Cr^{2+}:ZnSe. Initial progress in Cr:ZnSe mode-locked laser development consists of: active mode-locking of a Cr^{2+}:ZnSe laser with pulse duration of 2–4 ps [21], [22]; passive mode-locking of Cr^{2+}:ZnSe laser by a semiconductor saturable absorber mirror (SESAM) with pulse duration of $\sim$100 fs [23], [24]; Kerr-lens mode-locking (KLM) of Cr^{2+}:ZnSe laser with pulse duration of 95 fs [25]; energy scaling of a SESAM mode-locked Cr^{2+}:ZnSe fs oscillator in

Manuscript received April 1, 2014; revised July 21, 2014; accepted August 1, 2014. This work was supported by IPG Photonics Corporation and in part by the National Science Foundation under Grants ECS-0424310, EPS-0447675, BES-0521036, EPS-0814103, and ECCS-0901376, CBET-1321551, AFRL (Prime Contract No. FA8650–06-D-5401/0013, subcontract RSC09011), AFRL FA9451-10-C-0254 and AFOSR FA9550-13-1-0234.

S. B. Mirov, V. V. Fedorov, and D. Martyshkin are with the Center for Optical Sensors and Spectroscopies, Department of Physics, University of Alabama at Birmingham, CH 310, AL 35294 USA. (e-mail: mirov@uab.edu; vfedorov@uab.edu; dmartych@uab.edu).

I. S. Moskalev, M. Mirov, and S. Vasilyev are with the IPG Photonics, Mid-IR Lasers, Birmingham, AL 35203, USA (e-mail: imoskalev@ipgphotonics.com; mmirov@ipgphotonics.com; svasilyev@ipgphotonics.com).

Color versions of one or more of the figures in this paper are available online at http://ieeexplore.ieee.org.

Digital Object Identifier 10.1109/JSTQE.2014.2346512

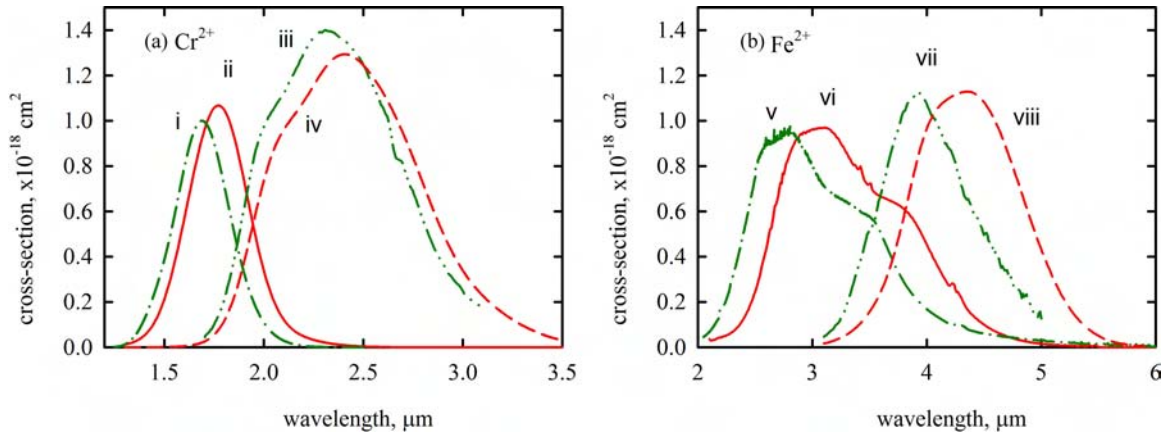

Fig. 1. (a) Absorption (Cr:ZnS- curve i; Cr:ZnSe-curve ii) and emission (Cr:ZnS- curve iii; Cr:ZnSe-curve iv) cross-sections of Cr^{2+} ions in ZnS and ZnSe; (b) Absorption (Fe:ZnS- curve v; Fe:ZnSe-curve vi) and emission (Fe:ZnS- curve vii; Fe:ZnSe-curve vii) cross-sections of Fe^{2+} ions in ZnS and ZnSe.

TABLE I
SPECTROSCOPIC CHARACTERISTICS OF CHROMIUM AND IRON IONS IN ZNS, ZNSE AT $^5T_2 \leftrightarrow {}^5E$ TRANSITIONS, σ_{ab}, σ_{em}, —PEAK ABSORPTION AND EMISSION CROSS-SECTIONS; λ_{ab}, λ_{em} —PEAK ABSORPTION AND EMISSION CROSS-SECTION WAVELENGTHS, RESPECTIVELY; $\Delta\lambda_{\mathrm{FWHM}}$ —FULL BANDWIDTH AT HALF MAXIMUM; τ_{rad} RADIATIVE LIFE TIME; $\tau_{\mathrm{RT}}(\tau_{77\mathrm{K}})$—LUMINESCENCE LIFETIME AT ROOM TEMPERATURE AND 77 K

	Cr^{2+}		Fe^{2+}	
	ZnS	ZnSe	ZnS	ZnSe
	Absorption			
σ_{ab}, 10^{-18} cm^2	1.0	1.1	0.92	0.97
λmax, μm	1.69	1.77	2.8	3.1
$\Delta\lambda_{\mathrm{FWHM}}$, μm	0.32	0.35	1.22	1.35
	Emission			
σ_{ab}, 10^{-18} cm^2	1.4	1.3	1.1	1.1
λmax, μm	2.35	2.45	3.94	4.35
$\Delta\lambda_{\mathrm{FWHM}}$, μm	0.82	0.86	0.91	1.13
τ_{rad}, μs	5.7	5.5	55–62	57
$\tau_{\mathrm{RT}}(\tau_{77\mathrm{K}})$, μs	4.3(5.7)	5.4	0.05(2.7)	0.38(57)

chirped-pulse regenerative amplifier with 0.3 mJ, 300 fs pulses and 1 GW peak power at a 1-KHz repetition rate [26].

Reported CW microchip and external cavity lasing of Cr^{2+}:ZnS [9]; demonstration of output powers in excess of 10 W [27]; diode pumped operation [28], [10]; early demonstration of SESAM [29], and more recent 1 W output power Kerr-Lens mode locked (KLM) [30], [31], as well as 41 fs graphene passive mode-locked operation [32]; all showed that Cr^{2+}:ZnS gain medium, being spectroscopically similar to Cr:ZnSe can serve as its viable alternative. Moreover, it has potential for providing higher power handling due to better hardness, higher thermal conductivity, higher thermal shock parameter, and lower thermal lensing [15], [27].

First tunable laser operation of Cr:$Cd_{0.85}Mn_{0.15}Te$ and Cr:CdSe lasers were realized in [33] and [34], respectively, soon after the first publications on Cr:ZnSe lasers. Further improvements in output characteristics of Cd chalcogenide lasers were demonstrated in [35] where an efficient Tm-fiber pumped Cr:CdSe laser operating at 2.6 μm with output power in excess of 1 W and 60% quantum slope efficiency was reported. In long (300 μs) pulse free running regime of excitation the same group achieved 2.26–3.61 μm tunability of the Cr:CdSe laser in a dispersive cavity, while reaching 17 mJ of output energy at 2.6 μm and 63% quantum efficiency in a nonselective cavity [36]. Overall, chromium doped Cd chalcogenides are appropriate for lasing at wavelengths up to 3.6 μm. However, due to a strong thermal lensing they are less attractive than Cr:ZnSe/S media for further power scaling at room temperature.

Pulsed low temperature lasing of Fe:ZnSe with output energy 12 μJ at 130 K and tunability over 3.98–4.54 μm [37] stimulated active interest to iron doped chalcogenides. First gain-switched lasing at room temperature was realized in [38]. The output energy in this regime was further scaled up to 5 mJ [39] and recently to 30 mJ [40]. Output energies in excess of 180 mJ at 85 K and 140 mJ for thermoelectrically cooled Fe:ZnSe were demonstrated under free running long-pulse (200 μs) Er:YAG 2.94 μm excitation [41], [42]. In [43] and [44] the output energy of a low temperature Fe:ZnSe laser was further scaled to 0.4 and 2.1 J, respectively.

Major physical and spectroscopic characteristics, methods of fabrication, as well as output characteristics of Cr and Fe doped II-VI chalcogenide mid-IR lasers are summarized in the following reviews with extensive list of references therein [15], [45]–[52]. In the following paragraphs we provide a review of recent studies aimed at the development of Cr and Fe doped ZnSe and ZnS lasers as the most promising for practical applications.

II. SPECTROSCOPIC PROPERTIES OF CR AND FE DOPED ZNSE/S COMPOUNDS

Spectroscopic properties of chromium and iron doped II-VI semiconductors have been studied for many decades and are summarized in several reviews and book chapters [15], [45]–[52]. In this section we updated some spectroscopic characteristics relevant to laser applications (see Fig. 1 and Table I). Both Cr^{2+} and Fe^{2+} ions have a ^{5}D ground state, which in the tetrahedral crystal field of II-VI semiconductors is split into $^5T_2$ triplet and ^5E doublet terms. The transitions between these

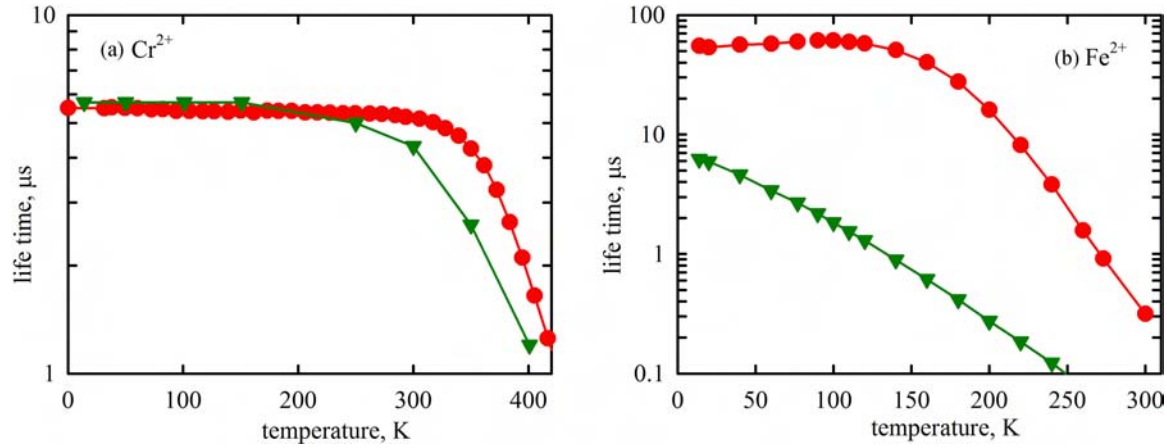

Fig. 2. Luminescence lifetime versus temperature for chromium (a) and iron (b) doped ZnS (triangle) and ZnSe (circle) crystals.

levels are in the mid-IR spectral region. All the transitions to other chromium and iron multiplets are spin forbidden.

Broad (1.5–2.1 μm) absorption bands and high Cr^{2+} ions absorption cross-sections ($\sim 10^{-18}$ cm^2) make possible direct optical pumping of ${}^5T_2 \rightarrow {}^5E$ transitions. Available pump sources include various diode, fiber and solid state lasers with pumping power of several hundred watts and energies of tens of joules.

Fig. 2 shows the temperature dependence of the mid-IR luminescence lifetimes of Cr:ZnS/ZnSe and Fe:ZnS/ZnSe crystals. The radiative lifetime of chromium transitions estimated from temperature dependences of lifetime as a low temperature limit were very close to each other ($\tau_{\mathrm{rad(Cr:ZnSe)}} = 5.5$ μs; $\tau_{\mathrm{rad(Cr:ZnS)}} = 5.7$ μs). Both chromium doped crystals reveal a high quantum yield of fluorescence at room temperature $\sim$1.0 and $\sim$0.8 for ZnSe and ZnS hosts, respectively. The emission cross-sections over 1.9–3.5 μm spectral range were calculated from the luminescence spectra and radiative lifetime measurements with the use of Füchtbauer-Ladenburg equation [53]. These favorable spectroscopic characteristics make Cr:ZnSe/ZnS crystals effective mid-IR gain media capable of lasing in many different regimes of oscillation at room temperature. Due to a smaller crystal field splitting of the ^{5}D multiplet of Fe^{2+} ions, the absorption and luminescence bands are shifted to longer wavelengths in comparison with chromium transitions (see Fig. 1 and Table I). The absorption cross section of the Fe:ZnSe was previously measured from absorption and saturation experiments (see ref [50] for details).

The peak RT absorption cross-section of Fe:ZnS crystal was calculated using data reported in [54]. The absorption cross-sections of the iron ions are very close to the absorption cross-sections of the chromium ions, however, the number of available optical pump sources with wavelength around 3 μm is limited. Also, as one can see from Fig. 2(b), the mid-IR luminescence of Fe^{2+} ions is thermally quenched at RT. The luminescence lifetimes were measured to be 380 and 50 ns for Fe:ZnSe and Fe:ZnS crystals, correspondingly [55]. This indicates that these crystals could efficiently oscillate in gain-switched regime at RT, but require cooling for effective CW lasing. As one can see from the Fig. 2(b), the radiative lifetime in Fe:ZnSe crystal could be estimated from the lifetime temperature dependence as $\tau_{\mathrm{rad}} = 57$ μs [55]. For Fe:ZnS crystal, the low temperature limit of the luminescence lifetime was measured to be 6.2 μs. It is close to the value of 5.5 μs reported earlier in [56]. The radiative lifetime of Fe in ZnS crystal cannot be estimated from the temperature dependence of the luminescence lifetime due to its quenching even at helium temperatures. The authors in [57] reported 10% of luminescence yield measured at low temperature in Fe:ZnS crystal. From these data points, one could estimate the radiative lifetime of Fe^{2+} ions in ZnS crystal as 55–62 μs, which is close to the value measured for Fe^{2+} ions in the ZnSe host.

The broad emission cross-sections of Fe in ZnS and ZnSe covering 3–5.5 μm spectral range were calculated from the luminescence spectra and radiative lifetime measurements with the use of Füchtbauer-Ladenburg equation and are depicted in Fig. 1(b).

Together the emission of these gain media cover spectral range between 1.9 and 5.5 μm, which is important for many medical, environmental, military and technological applications.

III. Cr:ZnSe/S Lasers

A. CW Tunable Cr:ZnSe/S Lasers

In this section we review our most recent developments in high-power CW tunable and single-frequency lasers based on Cr^{2+}:ZnS and Cr^{2+}:ZnSe gain materials.

Previously we reported on power scaling of CW tunable lasers based on Cr^{2+}:ZnS, Cr^{2+}:ZnSe gain media [47]. We demonstrated that conventional cavities based on Brewster configuration of the gain elements suffer severely from non-symmetric thermal lensing effects, which strongly limit the achievable output power and beam quality [27]. Recent progress in improving optical quality of polycrystalline Cr^{2+}:ZnS, Cr^{2+}:ZnSe slab gain elements and development of strong and reliable AR coatings for these materials allowed us to move to normal incidence linear resonator configurations.

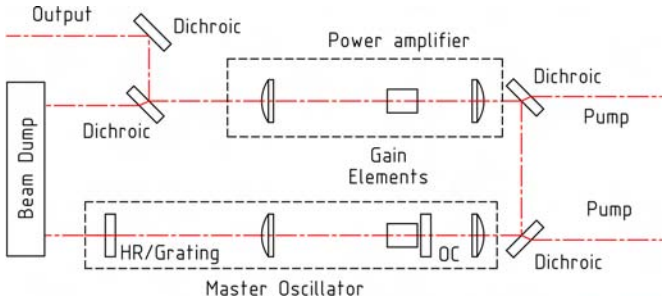

Fig. 3. Optical scheme of high-power tunable Cr^{2+}:ZnS and Cr^{2+}:ZnSe CW MOPA systems based on linear cavity design. In tunable lasers the HR end mirror is replaced with diffraction gratings in Littrow mount configuration. Single-frequency systems utilize Littman scheme. Single-pass power amplifiers are used to boost output power. Combination of these two gain materials in one system (i.e., Cr^{2+}:ZnS for master oscillator and Cr^{2+}:ZnSe for power amplifier) allows for considerable extension of wavelength tuning range.

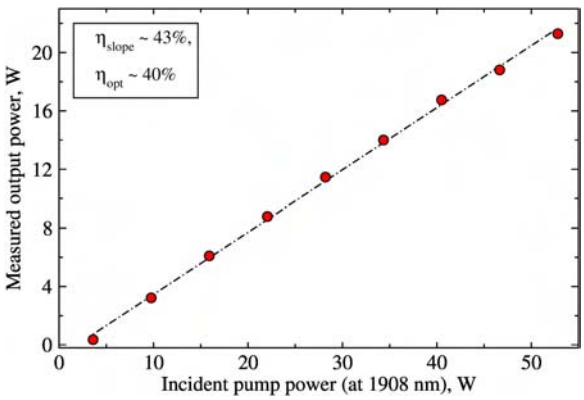

Fig. 4. Performance of Cr^{2+}:ZnS master oscillator at 2.4 μm pumped by a 50 W Tm fiber laser.

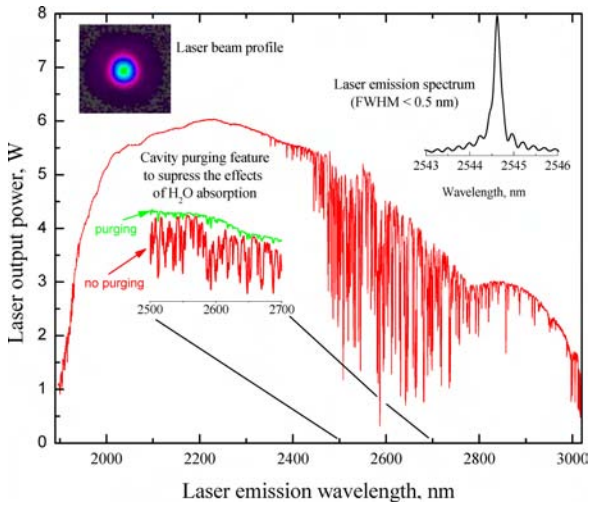

Fig. 5. Typical tuning curve of high-power, narrow-line tunable Cr^{2+}:ZnS/Se laser system. Intracavity water vapor absorption in the 2.5–2.7 μm spectral range leads to laser power suppression at certain wavelengths which can be mitigated by cavity purging.

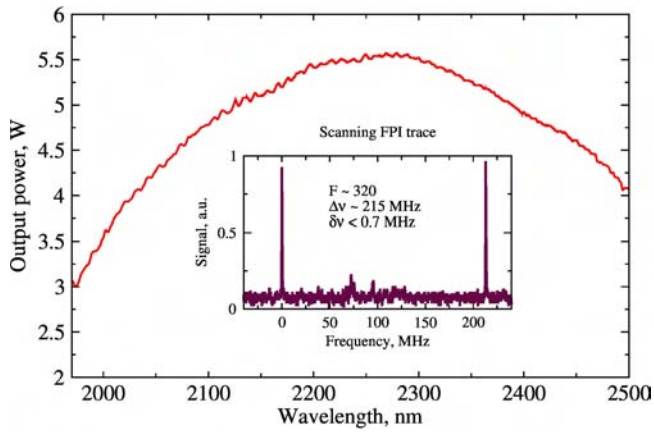

Fig. 6. Output power versus wavelength of a tunable single-frequency Cr^{2+}:ZnS/Se laser system. The insert shows an interferogram obtained with high-resolution ring interferometer. The upper estimate of the laser linewidth, limited by the interferometer resolution, is less than 0.7 MHz. The tuning is performed automatically using built-in motorized wavelength tuning mechanism.

The most general optical scheme of our CW tunable MOPA laser systems is shown in Fig. 3. These systems are usually pumped by either Er-fiber lasers at 1567 nm (preferable for Cr^{2+}:ZnS gain medium) or Tm-fiber lasers at 1908–1940 nm (more suitable for Cr^{2+}:ZnSe gain material). The gain elements have ultra-broadband AR coatings which span 1500–3200 nm spectral range.

The normal incidence configuration allows for obtaining previously unachievable levels of output power in the 2–3 μm mid-IR spectral region. Fig. 4 shows input-output characteristic of a Cr^{2+}:ZnS standalone master oscillator pumped by 50 W Tm fiber laser. This very simple mid-IR master oscillator uses 50% output coupler and operates near Cr^{2+}:ZnS gain maximum located near 2.4 μm. It is noteworthy that this input-output curve shows no rollover even at the maximum pump power. In our recent preliminary experiments we reached 30 W output power level using multi-element MOPA. It is expected that further increase of the pump power and beam combining techniques will allow for reaching 100 W output power levels within this very important mid-IR spectral region. One of the most important practical applications of 2.4 μm lasers is processing of polymer materials which have a large number of strong absorption lines near this wavelength (e.g., polypropylene, polycarbonate, PLA, PVA, PAC, COP and others.).

There are numerous applications where tunable mid-IR lasers are preferable to fixed-wavelength systems. Spectroscopic applications, testing of optical devices, material processing applications development, dynamic process monitoring; all require the broadest possible wavelength tuning ranges. Depending on the linewidth requirements, several methods are used to obtain wavelength tunable output: intracavity prism (typical linewidth is $<$5 nm); diffraction grating in the Littrow-mount configuration (linewidths are $<$1 nm and $<$0.1 nm without- and with intracavity prismatic beam expansion, respectively). A diffraction grating in the Littman scheme is used for obtaining single-longitudinal mode of operation. Typical tuning ranges for various lasers are shown in Figs. 5 and 6.

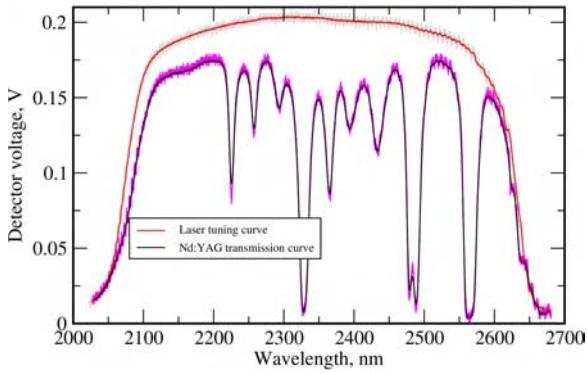

Fig. 7. Performance of rapidly tunable laser. The unidirectional sweep rate is 1 kHz (1000 spectra per second). The plots show laser tuning curve and transmission through a long Nd:YAG rod.

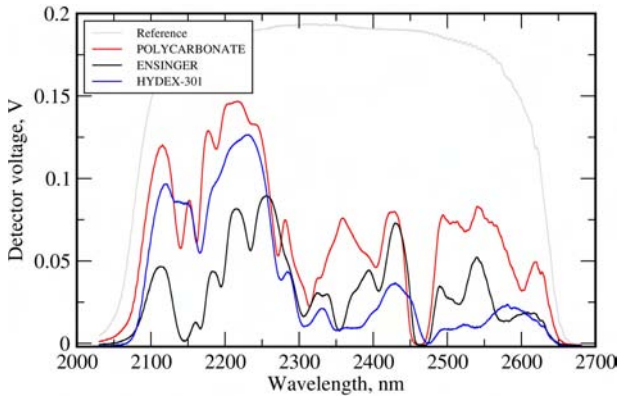

Fig. 8. Transmission curves of polymer (polycarbonate, polyphenylene/ensinger, polyurethane/hydex-301) samples obtained with the rapidly tunable laser module at 1 kHz sweep rate. This measurement illustrates the potential of the rapidly-tunable mid-IR laser systems for applications where fast dynamic spectral analysis is required (e.g., environmental monitoring, real-time process control).

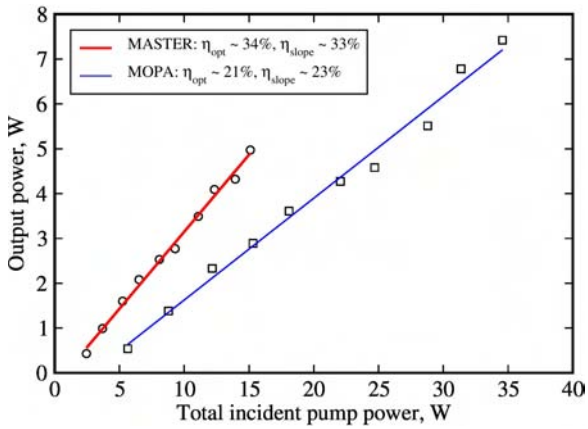

Fig. 9. Performance of Cr^{2+}:ZnSe, CW 2.94 μm laser system. The laser is built using the design shown in Fig. 3. The output wavelength of 2.94 μm is forced by using specially designed input and output mirrors with high transmission over entire 1.5–2.93 μm spectral range and high reflectivity at 2.94 μm. The laser is pumped by 50 W Tm fiber laser operating at 1908 nm central wavelength.

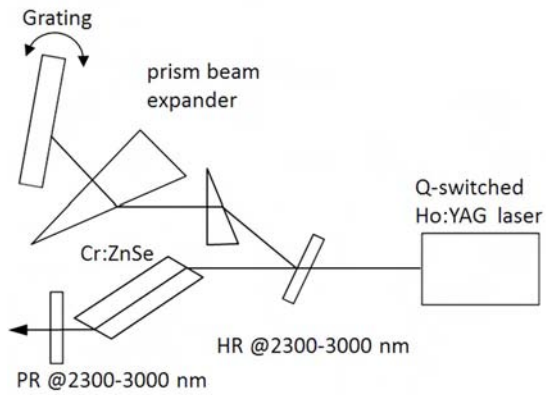

Fig. 10. Schematic of tunable gain switched Cr:ZnSe laser.

In our conventional tunable mid-IR lasers the wavelength tuning is performed using motorized tuning mechanisms actuated by precision stepper motors. This approach allows precise and repeatable wavelength setting as well as continuous wavelength scanning. However, this mechanism is relatively slow (~200 nm/s at the highest motor speed). There are a number of applications where fast wavelength scanning over the entire laser tuning range is highly desirable. For such applications we have developed a rapidly tunable laser system. The module is based on similar cavity design as shown in Fig. 3, but with a slightly different wavelength tuning approach: a high-speed octagon mirror scanner is installed into the mode path between the intracavity lens and a Littrow-mounted diffraction grating, which is used as an end mirror. This method allows for fast wavelength sweeps across the entire tuning range. Typical output spectra from the rapidly-tunable laser are shown in Figs. 7, and 8, where some examples of practical applications of this laser system are also demonstrated.

There is a great demand for a high-power CW laser systems operating at 2940 nm wavelength. In addition to the applications in medicine (where this wavelength is FDA approved), there is a very large potential for these systems in industrial applications for processing of various types of glasses and polymer materials. Due to relatively low gain of Cr^{2+}:ZnS and Cr^{2+}:ZnSe gain media at this wavelength and their inherently high thermo-optic coefficient (dn/dT); it has been a challenging task to upscale the output power of the CW 2.94 μm laser system. Our most recent results are depicted in Fig. 9.

Further power scaling of the 2.94 μm laser is limited by thermal lens effects in the gain media and requires more advanced approaches (such as various beam combining techniques).

B. Gain-Switched Cr:ZnSe/S Lasers Operating at High (>100 Hz) Repetition Rate

A schematic diagram of tunable gain-switched (GS) Cr:ZnSe laser is shown in Fig. 10. We used Q-switched Ho:YAG laser operating at 2090 nm as a pump source (see Section IV-B for details). The Ho:YAG laser was operating at 100–1000 Hz repetition rates with pulse energy over 5–15 mJ range and 15–50 ns

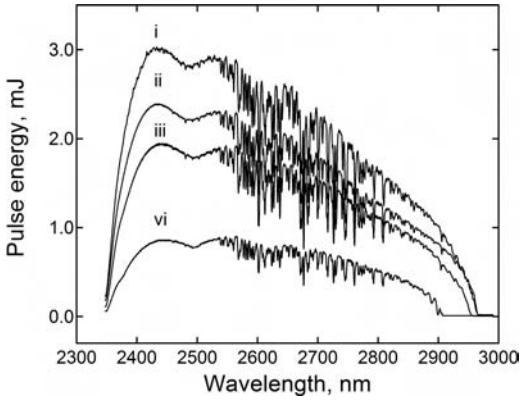

Fig. 11. Tuning curves of tunable gain switched Cr:ZnSe laser at different frequencies of operation: (i) 100 Hz, (ii) 300 Hz, (iii) 500 Hz, and (vi) 1000 Hz. Sharp dips at 2550–2800 nm are due to intracavity atmospheric water vapor absorption.

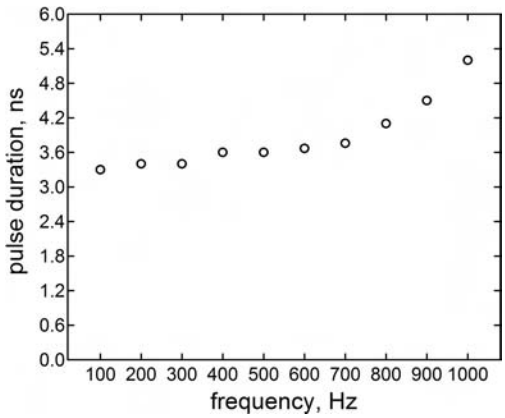

Fig. 12. Pulse duration versus pulse repetition rate at 2450 nm.

pulse duration. The GS laser cavity consists of a high efficiency (>90%) diffraction grating used in auto-collimation (Littrow) configuration, prism beam expander, HR folding mirror, Brewster-cut Cr:ZnSe crystal, and output coupler (R∼50%). The prism beam expander is used to prevent optical damage of diffraction grating as well as to provide narrow band laser oscillations. The bandwidth of laser radiation was less than 0.5 nm.

Output characteristics of GS Cr:ZnSe laser at different repetition rates are shown in Fig. 11. We achieved wavelength tuning over 2350–2960 nm spectral range at low repetition rates (100–400 Hz, see Fig. 11), and over 2350–2900 nm at higher repetition rates, (800–1000 Hz). Tunability at shorter wavelength was limited by reflection of folding mirror. In general it was possible to tune this laser over 1900–3000 nm spectral range with a shorter pump wavelength, e.g., 1645 nm Q-switched Er:YAG laser, and a proper set of mirrors. It is noteworthy that sharp dips in the tuning curves in Fig. 11 are due to intracavity absorption by atmospheric water vapor, which can be mitigated by cavity purging with dry Ar or N_2.

The pulse duration was in 3.3–5.3 ns range depending on repetition rate, as shown in Fig. 12.

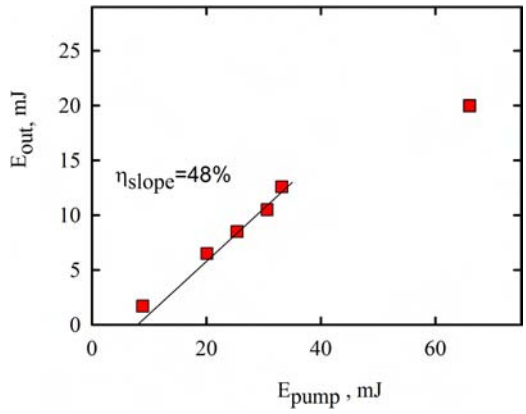

Fig. 13. Output-input characteristic of the gain switched (10 ns pump pulse duration) Cr:ZnSe laser.

C. Gain-Switched Cr:ZnSe/S Lasers Operating at Low (<100 Hz) Repetition Rate

Diode and/or flash-lamp pumped Q-switched solid state lasers can be utilized as Cr:ZnSe/S pump sources for high energy and low repetition rate applications. Output energy of 20 mJ from the single Cr:ZnSe oscillator was demonstrated using experimental set-up reported in [58]. For these experiments a Raman shifted Q-switched Nd:YAG laser with a repetition rate of 10 Hz, and pulse duration of 7 ns was used as a pump source for Cr:ZnSe laser oscillator. The Stokes line at 1.906 μm with maximum output energy of 300 mJ and pulse duration of 7 ns at FWHM; was realized with a H_2 Raman cell pumped in a backscattering geometry.

The Cr:ZnSe laser cavity was formed by a dichroic input mirror and the output facet of the Cr:ZnSe crystal with Fresnel reflectivity $R = 17\%$. The intracavity lens ($F_{ic} = 1$ m) increases energy density of the pump in the Cr:ZnSe gain elements, and helps avoid high energy density in the dichroic mirror. In addition, this lens provides stability of the Cr:ZnSe laser cavity. Gain element consisted of two Cr:ZnSe rectangular shaped crystals with a total beam propagation length of 8.2 mm and initial transmission ∼1% at 1.9 μm. The gain element was longitudinally pumped though the input mirror. The input-output dependence is shown the Fig. 13.

As one can see from the Fig. 13 the slope efficiency was equal to 48%. The limiting factor in this experiment was the optical damage of the input mirror. Optimization of the pump beam diameter at the input mirror enabled $E = 20$ mJ output energy at 66 mJ incident pump energy.

A gain-switched Cr:ZnSe MOPA system was recently reported in [59]. Diode pumped Tm:YAG lasers with acousto-optical Q-switch operating at 2.01 μm with 10 Hz rep rate were used to pump a tunable Cr:ZnSe MOPA system. The oscillation wavelength of the Cr:ZnSe master oscillator was tunable by acousto-optic filter within 2.12–2.7 μm spectral range. The laser cavity was designed in a Z-shaped configuration using a 7.5 mm Brewster cut Cr:ZnSe crystal with chromium concentration $N = 5.5 \times 10^{18}$ cm^3 and 60% reflectivity of the output coupler. The maximum output energy of 4.8 mJ at 2.43 μm was

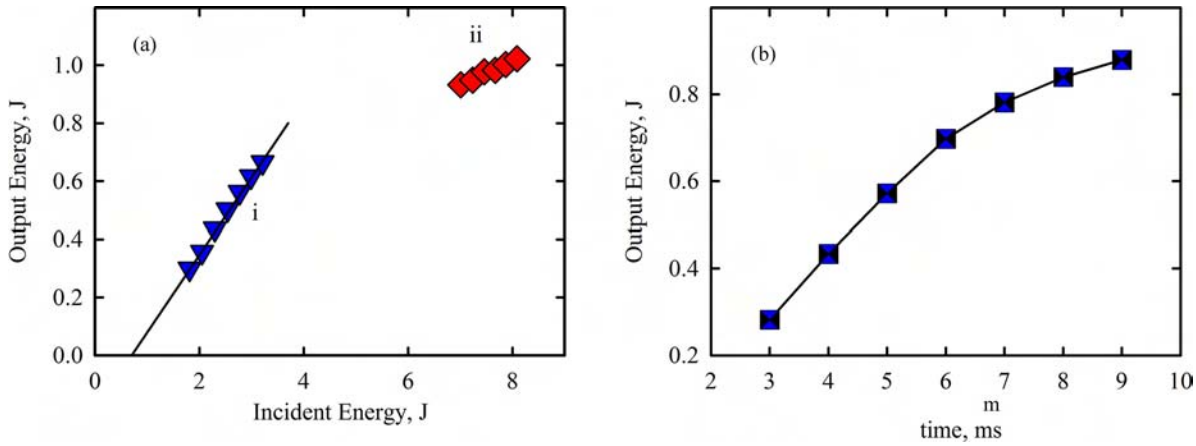

Fig. 14. (a) Output-input characteristic of the Cr:ZnSe laser measured for 5 ms (i) amd 7 ms (ii) pump pulse duration; (b) Output energy of the Cr:ZnSe laser versus pulse duration of Er-glass pump laser.

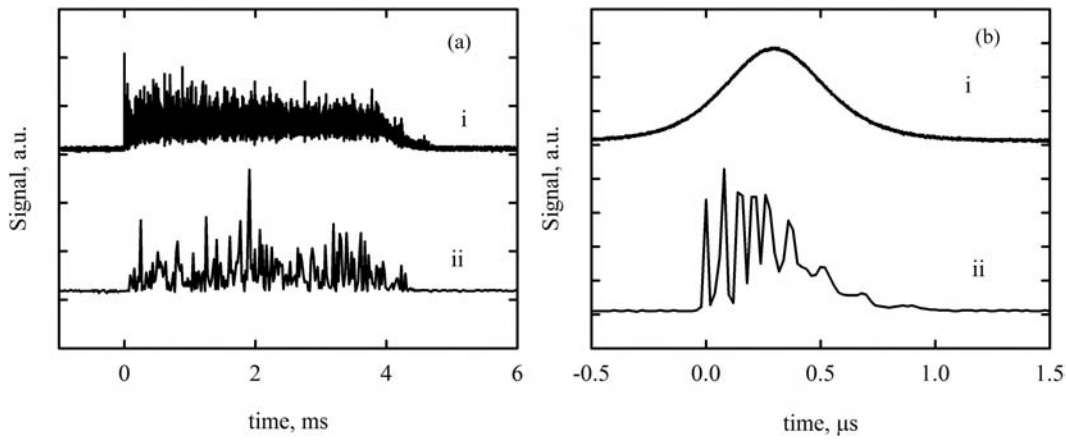

Fig. 15. (a) Temporal profiles of the pump (i) and Cr:ZnSe (ii) pulses. (b) Temporal profiles of single spike of the pump (i) and Cr:ZnSe (ii) lasers.

obtained under 16 mJ pump energy. The three stage Cr:ZnSe power amplifier was studied in the paper. The Cr:ZnSe crystals used in the amplifier were 5×7 mm^2 in aperture, 15 mm long, and had chromium concentration $N = 9 \times 10^{18}$ cm^3. The output energies were measured to be 13.8, 30.5, and 52.2 mJ with conversion efficiency of 39.2%, 46.6%, and 44.4% in first, second, and third stage amplifier, respectively. This Cr:ZnSe MOPA system was further used for pumping of a 6–10 μm tunable ZGP OPO system.

D. Free Running Cr:ZnSe Lasers

There are several important applications that require significantly higher output energy in longer pulses without special requirements for output beam characteristics. A compact 1 J mid-IR Cr:ZnSe Laser was recently reported in [60]. An Er-glass laser operating at 1.54 μm with 0.1–1 Hz repetition rate, and pulse duration variable over 3–10 ms (Palomar Lux1540) was used as a pump laser for such a Cr:ZnSe laser system. Output radiation of the Er-glass laser was coupled to an optical fiber with $\mathrm{N.A.} = 0.15$. The 9 mm long Cr:ZnSe laser cavity consisted of a 10 cm radius-of-curvature concave input mirror and a flat output coupler (R$\sim$60%). Pump radiation was focused into 5 mm long AR coated Cr:ZnSe gain element with 8×10^{18} cm^{-3} chromium concentration.

In the preliminary experiments, a Cr:ZnSe laser was characterized under 5 ms pump pulse excitation. This Cr:ZnSe laser demonstrated 0.7 J of output energy, and 27% slope efficiency with respect to the incident pump energy (see Fig. 15(a)). Fig. 15(a) shows envelopes of the pulses in ms-time scale. The pulses overlap and don't reveal any thermal roll-off at the end of the oscillation. However, fine structures of the pump and oscillation pulses are different. The pump pulses demonstrate relaxation oscillation over the whole pulse duration with modulation depth of approximately 50% after the first spike, and 5 μs average period of oscillation. The Cr:ZnSe laser pulse consists of separate lasing spikes with pulse duration around $\sim$1 μs. Moreover, individual spike of the Cr:ZnSe laser reveals its own relaxation oscillation with time between spikes $\sim$100 ns (see Fig. 15(b)). The time-resolved oscillation spectra are shown in Fig. 16. Oscillation wavelength was centered at 2.65 μm and spectral linewidth was 50 nm FWHM. The output of the Cr:ZnSe

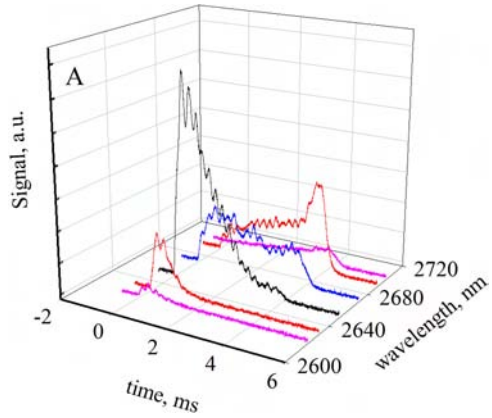

Fig. 16. The time-resolved oscillation spectra of the Cr:ZnSe laser.

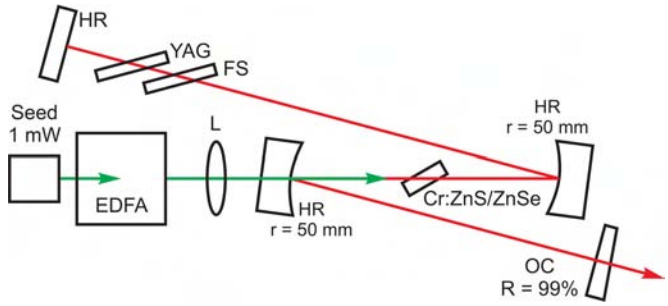

Fig. 17. Schematic of the Kerr-lens mode-locked polycrystalline Cr^{2+}:ZnSe/ZnS laser. HR—high reflectors, OC—output coupler, FS, YAG—dispersion compensation plates, L—pump focusing lens. The laser is pumped at 1550 nm by a radiation of narrowband semiconductor laser (seed) amplified to 1—2 W in Er-doped fiber amplifier (EDFA).

laser was observed to have a small shift to longer wavelengths at the end of the oscillation pulse. The dependence of the output energy of Cr:ZnSe laser for different pulse duration is depicted in Fig. 14(b). The output energy remains linear up to 6 ms pulse duration. A small roll-off due to thermal effect was observed for the pulse duration longer than 7 ms. The output energy of Cr:ZnSe laser under 7 ms pulse duration is shown in Fig. 14(a). The maximum output energy of the Cr:ZnSe laser was measured to be 1.1 J. The output beam was collimated into 4 mm diameter with divergence of ~30 mrad.

E. Femtosecond Polycrystalline TM:II-VI Lasers

Recent efforts on ultrafast Cr^{2+}:II-VI oscillators were concentrated on further improvement of the laser parameters in terms of reliability, average power and pulse duration. It was understood that the use of SESAM imposes limits on the output laser power and pulse duration. Therefore, the interest has been centered on the development and optimization of pure Kerr-lens mode-locked oscillators [30], [61], [62]. It was demonstrated that Cr^{2+}:ZnS is a promising material for mid-IR ultrafast lasers. On the one hand, Cr^{2+}:ZnS and Cr^{2+}:ZnSe have similar spectroscopic and laser parameters. On the other hand, Cr^{2+}:ZnS has higher thermal conductivity, higher thermal shock parameter and lower thermal lensing. Kerr-Lens mode-locked Cr^{2+}:ZnS laser with 1 W output power in harmonic mode-locking regime (the pulse repetition rate twice as high as the cavity mode spacing) laser has been recently reported [31]. The mid-IR pulses of only 5.1 optical cycles (41 fs) with 190 nm spectral bandwidth, 250 mW average output power at 108 MHz repetition rate were reported for graphene mode-locked Cr:ZnS laser [32].

Reliability and reproducibility of ultrafast Cr^{2+}:II-VI lasers depend on availability of the gain elements with high optical quality and uniformity of the laser properties. Until very recently, it was widely believed that KLM regime in Cr^{2+}:ZnSe/ZnS lasers requires the use of single crystal gain medium. Currently, high quality Cr^{2+}:ZnS and Cr^{2+}:ZnSe single crystal materials are not readily available. Crystal sublimation during the growth process results in poor uniformity of the single-crystal samples and limits the dopant concentration. It is often required to locate a 'good spot' inside the single crystal in order to achieve KLM regime of the laser.

An important advantage of polycrystalline Cr^{2+}:ZnS/ZnSe laser media is the post-growth diffusion doping technology, which enables mass production of large-size laser gain elements with high dopant concentration, uniform dopant distribution, and low losses. Results in polycrystalline Cr^{2+}:ZnS/ZnSe crystals have gradually superseded single-crystals in cw, gain-switched, and SESAM-mode-locked regimes of laser operation. The recent demonstration of KLM in polycrystalline Cr^{2+}:ZnS/ZnSe [63] is an important milestone and opens new venue for the development of commercial ultrafast mid-IR lasers.

Polycrystalline Cr^{2+}:ZnS/ZnSe laser gain elements are produced by thermal diffusion doping of chemical vapor deposition (CVD) grown polycrystalline ZnS and ZnSe [47]. Post-growth diffusion doping of CVD-ZnS/ZnSe retains the polycrystalline zinc-blend structure of the material with the grain size of 50–100 μm.

Zinc-blende II-VI semiconductors (ZnSe, ZnS, ZnTe) exhibit rather high second-order nonlinear susceptibility, which exceeds the values of birefringent materials such as ammonium dihydrogen phosphate (ADP) and potassium dihydrogen phosphate [64]. Furthermore, the grain size in CVD-ZnS/ZnSe is of the order of the coherence length of SHG process in the mid-IR wavelength range. This feature of polycrystalline Cr^{2+}:ZnS/ZnSe laser media is of importance in fs laser regime, as will be discussed below.

In this section we give an overview of our recent results on ultrafast polycrystalline Cr^{2+}:ZnSe/ZnS lasers. The spectral and temporal parameters of the lasers were characterized using a grating monochromator with ~0.5 nm resolution and an interferometric autocorrelator equipped with a pair of oppositely mounted 3-mm thick dielectric coated beam splitters (YAG), gold mirrors with SiO_2 protective layer, and a two-photon Ge detector. The autocorrelator was built in house. Therefore, our evaluations of the pulse duration are approximate for very short pulses.

Schematic of the first reliable polycrystalline Cr^{2+}:ZnSe/ZnS KLM laser is shown in Fig. 17. The output of a linearly polarized

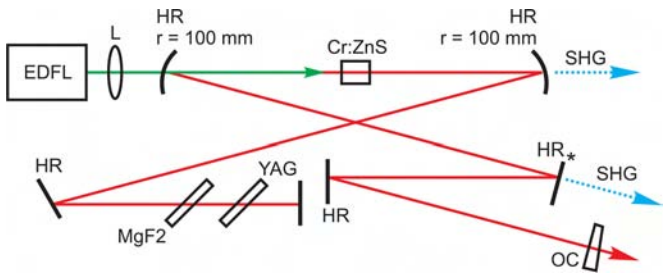

Fig. 18. Schematic of Cr^{2+}:ZnS KLM laser with optimized resonator. HR – dispersive high reflectors (GDD ~ -200 fs^2), YAG—2 mm thick Brewster mounted dispersion compensation plate, OC—output coupler (|GDD| < 150 fs^2), MgF_2—optional 0.5 mm thick Brewster mounted birefringent tuner (Lyot filter), L—pump focusing lens. SHG—secondary outputs of the laser at SH wavelength. The laser is pumped at 1567 nm by a linearly polarized radiation of Er-doped fiber laser (EDFL).

Er- doped fiber amplifier (EDFA) seeded by a low noise 1550 nm narrowband semiconductor laser was coupled to the standard astigmatism compensated asymmetric Z-folded resonator consisting of two curved high reflecting (HR) mirrors, plane HR mirror and plane output coupler (OC, $R = 99\%$). The length of the laser cavity was about 94 cm. KLM regime was obtained using two types of laser media: polycrystalline Cr^{2+}:ZnS (2.0 mm thick, 43% low-signal transmission at 1550 nm) and polycrystalline Cr^{2+}:ZnSe (2.4 mm thick, 15% transmission). Gain elements were plane-parallel polished, uncoated and Brewster mounted on a copper heat sink without forced cooling. The cavity mirrors were non-dispersive. The dispersion compensation was implemented using a combination of Brewster mounted fused silica plate (2 mm thick) and YAG plate (4 mm thick). The group delay dispersion of the resonator at 2400 nm, near the central laser wavelength, was about -1000 fs^2.

The laser was optimized for maximum CW output power and then the distance between the curved mirrors was fine-adjusted in order to obtain KLM regime. The mode-locked laser oscillation was initiated by translation of the OC.

Multi-hour uninterrupted single-pulse oscillations were observed in Cr^{2+}:ZnSe at 1 W pump power and 60 mW laser output power. Further increase of the pump power resulted in multi-pulsing and frequent interruptions of the mode-lock. The emission of Cr^{2+}:ZnSe laser was chirped with the approximate pulse duration of 130 fs.

Maximum stability of Cr^{2+}:ZnS KLM laser was observed at 1.25 W pumping and 30 mW output power (1–2 h of uninterrupted single-pulse oscillations). The output of Cr^{2+}:ZnS laser was sech^2 transform limited with 125 fs pulse duration.

To improve the output characteristics of polycrystalline mid-IR laser in KLM regime we (i) optimized the parameters and mounting of the gain element, (ii) optimized the design and dispersion of the laser resonator, (iii) optimized the OC transmission. These optimizations allowed us to significantly increase the laser output power in KLM regime and to produce shorter pulses.

Schematic of the optimized laser is shown in Fig. 18. As a pump source, we used a linearly polarized Er-doped fiber laser (EDFL). In order to increase the laser output power and efficiency of lasing we used a 5 mm long polycrystalline Cr^{2+}:ZnS gain element with 11% low-signal transmission at 1567 nm pump wavelength. The gain element was AR coated and mounted in the resonator at normal incidence on a water cooled copper heat sink. The main advantages of normal incidence mounting of the gain element are (i) better management of the thermal optical effects in the gain element due to circularity of the pump and laser beams, (ii) significant increase of pump and laser intensity inside the gain element (if compared with the standard Brewster mounting), (iii) ability to use gain elements with large length and, hence, high pump absorption. Normal incidence mounting may also be more favorable for Kerr-lens mode-locking [65].

TABLE II
OUTPUT CHARACTERISTICS OF THE OPTIMIZED Cr^{2+}:ZNS KLM LASER

R_{OC}, %	P_{out}, W	τ, fs	$\Delta\lambda$, nm	λ_C, nm	P_{pump}, W
96	0.3	85	70	2380	3.4
90	0.6	46 *)	120 *)	2300	5.2
70	1.2	68 *)	84 *)	2332	6.7
50	2.0	67	82	2295	10.0

R_{OC} – reflectivity of the output coupler, P_{out}—average output laser power in KLM regime, τ - laser pulse duration (FWHM), $\Delta\lambda$—width of the laser emission spectrum (FWHM), λ_C—laser emission peak, P_{pump} – optimal pump power. *) – conservative estimates of the spectral bandwidth and of the pulse duration.

The lengths of the cavity legs were unequal with a typical ratio of 2:5. The angles of incidence at the curved HR mirrors were minimized in order to reduce the astigmatism of the resonator. Dispersion management was implemented by the use of dispersive high reflectors (GDD ~ -200 fs^2 in 2200—2500 nm range) and 2 mm thick Brewster mounted YAG plate. Dispersion of the OCs was within ± 150 fs^2 in 2200–2400 nm range. Overall dispersion of the resonator at the maximum of laser emission (2300–2400 nm) was about -1400–1600 fs^2. For the experiments on wavelength tuning of the KLM laser we used a 0.5 mm thick MgF_2 Brewster mounted birefringent tuner (single-plate Lyot filter).

KLM regime of the laser with the optimized resonator was obtained using output couplers with 96%, 90%, 70%, and 50% reflectivity. Most measurements were carried out at the pulse repetition rate of 94.5 MHz. However, KLM laser oscillations were obtained in a range of pulse repetition rates (80–120 MHz). Results of the laser characterization are summarized in Table II.

The laser parameters, shown in the table, correspond to the single pulse oscillations at 94.5 MHz repetition rate and multi-hour uninterrupted laser operation in Kerr-lens mode-locked regime. The highest average power of KLM laser was obtained with $R_{OC} = 50\%$: 2 W with 67 fs pulse duration which corresponds to 21 nJ pulse energy and 275 kW peak power. The shortest pulse duration, with the conservative estimate of 46 fs, was obtained at 0.6 W average output power using $R_{OC} = 90\%$. Right column in Table II shows the optimal pump power for different OCs. Optimization of the pump power was essential as an increase of the pump by 10–15% above the optimum resulted in unstable pulsing, multi-pulsing and spikes in the laser emission spectrum.

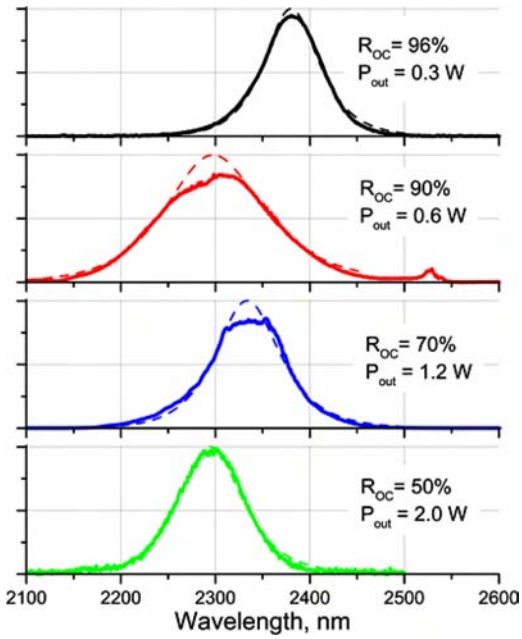

Fig. 19. Emission spectra of KLM laser with different reflectivity ($R_{\rm OC}$) of the output coupler. Dashed lines show sech fit of the spectra.

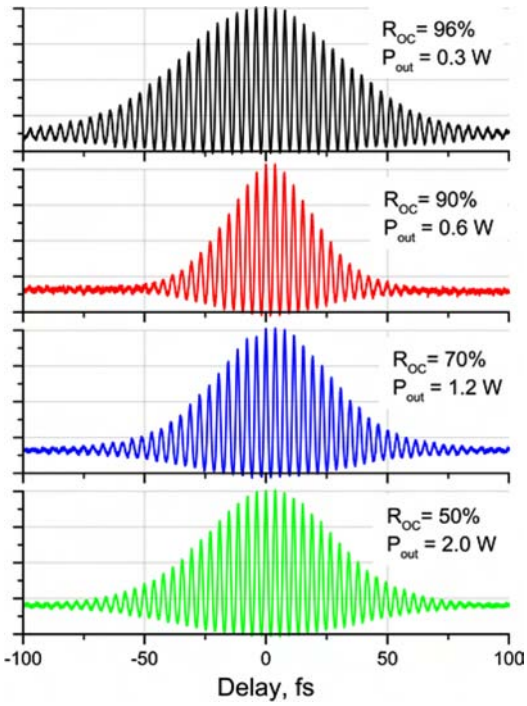

Fig. 20. Autocorrelation traces of KLM laser with different reflectivity ($R_{\rm OC}$) of output coupler.

Emission spectra and autocorrelation traces of KLM laser obtained for the OCs with different reflectivity are illustrated in Figs. 19 and 20, respectively. The shape of the spectra and of the autocorrelation functions correspond to sech^2 pulses for $R_{\rm OC} = 96\%$ and $R_{\rm OC} = 50\%$. This allows us to use the time bandwidth product of 0.315 for estimation of the pulse duration. The emission spectra, measured for $R_{\rm OC} = 90$ and 70%, are flat-top. Therefore, we used conservative estimates for the spectral bandwidth and the pulse duration. We explain the flat-top spectra by second harmonic generation (SHG) in polycrystalline Cr^{2+}:ZnS, as will be discussed below. We explain the small peak at 2525 nm in the spectrum measured for $R_{\rm OC} = 90\%$ by presence of Kelly sidebands in the laser emission, see, e.g., [25]. The opposite sideband is suppressed due to leakage through high reflectors at the wavelengths below 2200 nm.

Our experiments revealed a particular feature of polycrystalline Cr^{2+}: II-VI laser media: we observed generation of second, third and fourth optical harmonics of the fundamental mid-IR laser emission in femtosecond regime of polycrystalline Cr^{2+}:ZnS laser. The laser output power as high as 40 mW was measured at second harmonic (SH) wavelength for the $R_{\rm OC} = 96\%$. The SH power was measured behind one of the high reflectors (shown by asterisk on Fig. 18). Average transmission of the HR mirrors in SH wavelength range is about 50%. That allows estimating ~160 mW SHG power inside the resonator, in one direction. The typical SHG output power was about 30 mW for $R_{\rm OC} = 90\%$, 10–20 mW for $R_{\rm OC} = 70\%$, and 5–10 mW for $R_{\rm OC} = 50\%$. A decrease in the optical power inside the resonator resulted in decrease of SHG output. The output power of the KLM laser at third and fourth harmonics was at mW and μW levels, respectively.

Thus, a considerable fraction (up to 50%) of the mid-IR femtosecond laser emission can be converted to the SH and the amount of the SH power can be adjusted by control of the OC reflectivity. The observed strong SHG effect can be explained by polycrystalline structure of the material [66]–[68]. The size of the microscopic single-crystal grains is of the same order as the coherence length of the SHG process. Dissimilarities in the grain size and in orientation of the crystallographic axes result in the 'patterning' of the material, like in quasi phase matched (QPM) nonlinear converters. Unlike in the standard QPM material, the patterning is not regular but random. On one hand, the nonlinear gain in randomly patterned material is very low. On the other hand, random patterning results in very large bandwidth of the nonlinear frequency conversion. A linear dependence of the nonlinear yield on the thickness of randomly patterned medium has been predicted [67] and observed in the experiment [68]. Our observations show that low nonlinear gain of polycrystalline Cr^{2+}:ZnS is compensated by high intensity of fs laser pulses inside the resonator.

SHG effect has been routinely observed in SESAM mode-locked polycrystalline Cr^{2+}:ZnS/ZnSe lasers. Reported SHG signals were at sub-mW level (intracavity) or about 10^{-4} of the main signal [69]. We explain the significant increase of SHG signal in our experiments by specific features of the resonator: (i) mounting of the gain element at normal incidence, (ii) relatively large length of the gain element, (iii) significant increase of the optical power at fundamental mid-IR wavelength.

Typical images of the laser output beams at different wavelengths are shown in the top of Fig. 21 (the snapshots were made at 2 W KLM laser output, $R_{\rm OC} = 50\%$). Graph in the bottom of Fig. 21 shows a femtosecond pulse train at 94.5 MHz, acquired at SH wavelength by fast InGaAs photo-detector, installed behind one of the HR mirrors.

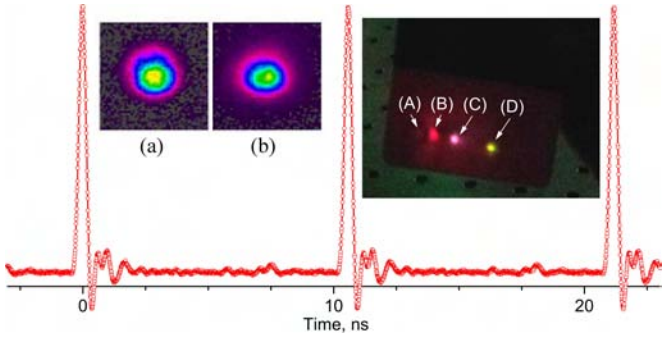

Fig. 21. Top: images of the fs laser output beams at fundamental (a), second (b), third (c) and forth (d) harmonic wavelengths (2300, 1150, 770, 575 nm, respectively). Two images on the left were acquired by a pyroelectric camera. Three beams on the right is a photo of IR-sensitive card placed behind the OC (collinear spectral components of the laser output were resolved by a dispersive prism). Bottom: waveform of the KLM laser pulse train acquired at SH wavelength by fast InGaAs photodetector.

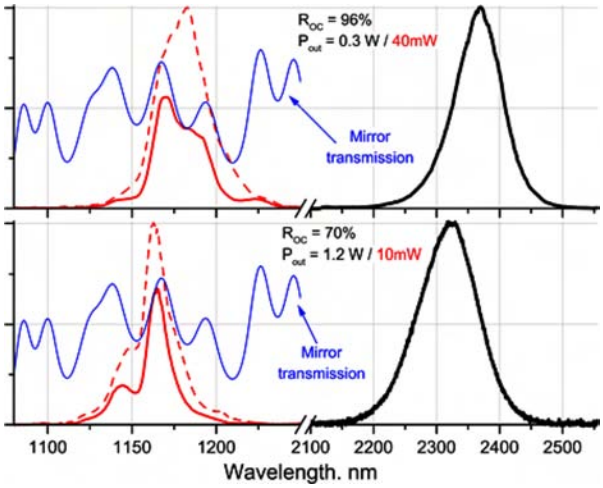

Fig. 22. Emission spectra of KLM laser: spectra on the right—fundamental wavelength spectra on the left—SH wavelength, solid lines—measured spectra, dashed lines—SHG spectra normalized to the mirror transmission (oscillating curves). Top graph: $R_{\rm OC} = 96\%$, laser output power $P_{\rm out} = 0.3$ W/40 mW (fundamental / SH wavelength). Bottom graph: $R_{\rm OC} = 70\%$, $P_{\rm out} = 1.2$ W/10 mW (fundamental / SH).

Emission spectra of KLM laser at fundamental and at SH wavelengths are compared in Fig. 22. Measurements were carried out for $R_{\rm OC} = 96\%$ (top graph) and $R_{\rm OC} = 70\%$ (bottom graph). For the spectral measurement we used SHG output after the right curved HR mirror (see Fig. 18). SHG power was measured behind plane HR mirror (marked on Fig. 18 by asterisk). Measured SHG spectra (solid curves) were normalized to take into account the oscillations of the mirror transmission in SHG spectral range.

Normalized SHG spectra are shown in the graphs by dashed curves. SHG conversion in the 'closed' resonator ($R_{\rm OC} = 96\%$) resulted in rather uniform and broad SHG spectrum with FWHM bandwidth of 34 nm (versus 84 nm bandwidth at fundamental wavelength). Use of the output coupler with high transmission ($R_{\rm OC} = 70\%$) resulted in significant narrowing of SHG emission (21 nm SHG bandwidth versus 100 nm bandwidth at fundamental wavelength) and in distortions of SHG spectrum.

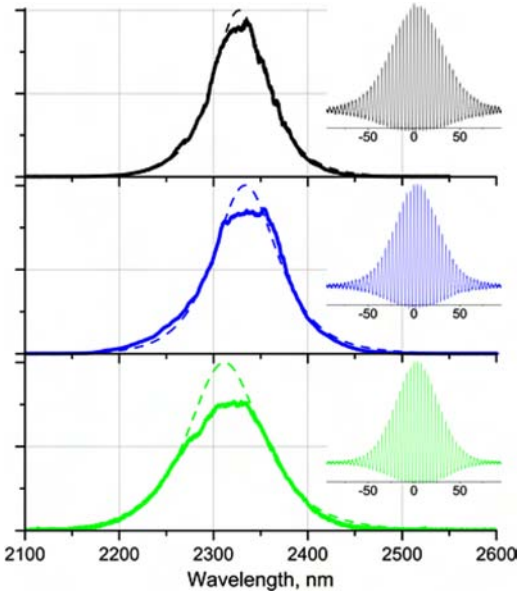

Fig. 23. Control of KLM laser parameters by translation of polycrystalline gain element along the waist of the laser beam. Emission spectra and the autocorrelation traces were measured for three different locations of the gain element (total translation along the waist within 0.5 mm). Dashed lines show the fit of measured spectra by sech profiles.

The Kerr effect is proportional to the optical intensity while SHG is quadric on intensity. Thus, the relative 'strengths' of two nonlinear effects can be adjusted by translation of polycrystalline gain element along the waist of the laser beam. Our experiments have shown that small translations of the gain element (by a fraction of its length) do not disrupt KLM regime of the laser and allow adjustment of SHG output power. Furthermore, translation of the gain element along the waist resulted in variation of width/shape of KLM laser emission spectrum and affected the laser pulse duration, as illustrated in Fig. 23.

The resonator was equipped with $R_{\rm OC} = 70\%$ output coupler. The spectra and autocorrelation traces of the KLM laser were measured for different locations of the gain element ($\sim$0.25 mm pitch). Displacement of the gain element resulted in significant increase of SHG output, from 10 mW (top graph) to $\sim$25 mW (bottom graph), while the laser output power was reduced from 1.2 to 1.0 W. In case of 'weak' SHG (top graph), the emission spectrum is rather close to sech profile with FWHM bandwidth of 68 nm and 84 fs pulse duration. In case of 'medium' SHG (middle graph) the emission spectrum has flattened, the spectral bandwidth has increased to 84 nm and the pulse duration has decreased to 68 fs. Further increase of the SHG 'strength' (bottom graph), resulted in more distorted spectrum with $\sim$95 nm bandwidth and $\sim$60 fs pulse duration. Thus, our observations show that translation of the gain element along the waist of the laser beam allows for adjustment of SHG power and can be used for fine-tuning of the ultrafast laser parameters at fundamental wavelength.

To implement wavelength tuning of the femtosecond laser, we equipped the resonator with a Brewster mounted 0.5 mm thick MgF_2 birefringent plate (Lyot filter), see Fig. 18. The broadest

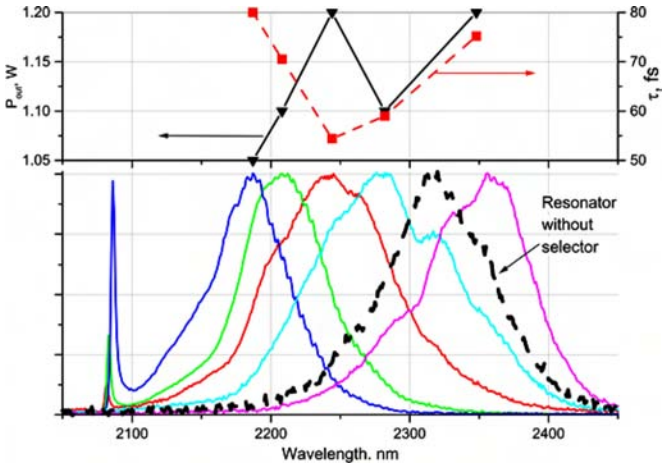

Fig. 24. Tuning of central wavelength of KLM laser by rotation of MgF_2 birefringent plate (Lyot filter). Top: dependences of average output power ($P_{\rm out}$, solid line, triangles) and pulse duration (τ, dashed line, squares) on central wavelength of KLM laser emission. Bottom: emission spectra of KLM laser in different parts of the tuning range (solid lines) and emission spectrum of KLM laser without the filter (dashed line).

tuning range was obtained for $R_{\rm OC} = 70\%$. The results of the experiment are summarized in Fig. 24. The single-plate birefringent tuner allowed tuning of the central wavelength within 2180–2360 nm range in KLM regime (the wavelength was tunable within 2150–2400 nm range in cw regime). Fine-alignment of the distance between the curved mirrors and re-initiation of KLM regime was required to tune the laser in the whole range. Continuous tuning of the laser with KLM regime maintained during tuning was obtained in the range of about 100 nm. Dependence of the laser output power on the wavelength is shown in the top graph by solid line. We explain the decrease of the output power at short wavelengths by a leakage through high reflectors. We also observed strong dependence of the laser pulse duration on the wavelength (top graph, dashed line). One can assume that the shortest pulse (2250 nm) corresponds to the optimal GDD of the resonator (-1320 fs^2, according to our calculations). Tuning of the laser wavelength below 2250 nm resulted in distorted spectra and chirped pulses. We explain this behavior by increase of GDD of high reflectors and of the gain element. In our opinion, obtained tuning range was mostly limited by insufficient selectivity of the MgF_2 birefringent tuner. Broadband tuning of fs laser may also require better dispersion management of the resonator (e.g., the use of the chirped dielectric mirrors).

In conclusion, our recent experiments have confirmed high suitability of polycrystalline Cr^{2+}:ZnSe and Cr^{2+}:ZnS media for generation of ultra-short laser pulses in mid-IR spectral range. Optimization of the parameters of the polycrystalline Cr^{2+}:ZnS gain element and the use of optimized laser resonator with dispersive dielectric mirrors has allowed us to obtain Kerr-lens mode-locked laser oscillations with 2 W average output power and sech^2 transform limited pulses with 67 fs pulse duration at 94.5 MHz pulse repetition rate.

Multi-hour uninterrupted laser operation in Kerr-lens mode-locked regime was observed in a standard lab environment.

We found that KLM laser regime is not sensitive to the location of the laser beam in the polycrystalline gain element. For instance, KLM regime is easily initiated after translation of the gain element across the resonator (i.e., in the direction perpendicular to the plane of Fig. 18). This confirms high uniformity of optical and laser properties of polycrystalline Cr^{2+}:ZnS/ZnSe. This feature of polycrystalline II–VI laser materials is of importance for practical use as it greatly simplifies the fs laser alignment.

We characterized a number of configurations of Kerr-lens mode-locked polycrystalline Cr^{2+}:ZnS laser:

1) Stable single-pulse fs laser oscillations were obtained in a range of the pulse repetition rates (80–120 MHz).
2) Highest output power of fs laser (2 W) was reached using the output coupler with 50% reflectivity.
3) Shortest pulse duration (about 46 fs) was reached at 0.6 W output power using the output coupler with 90% reflectivity.
4) Continuous tuning of Kerr-lens mode-locked laser within 100 nm range at $\sim$1 W output power was implemented using a MgF_2 birefringent tuner and an output coupler with 70% reflectivity.
5) We observed efficient conversion of the whole mid-IR laser emission spectrum to the SH in the polycrystalline Cr^{2+}:ZnS gain element. We estimate the SHG power as high as 160 mW inside the resonator, in one direction, at 96% reflectivity of the output coupler.
6) We demonstrated that the parameters of Kerr-lens mode-locked polycrystalline Cr^{2+}:ZnS laser (pulse duration, spectral bandwidth, SHG output power) can be fine-tuned by translation of the gain element along the waist of the laser beam

Further research is required to understand the implications of the surprisingly strong second order nonlinear effects in polycrystalline TM:II-VI laser gain media, in ultrafast laser regime. It is unclear whether the coupling between Kerr nonlinearity and second order nonlinearity of the gain medium is strong enough to affect the dynamics of the ultra-fast laser.

Apart from observed SHG and sum frequency generation, one can also expect the effects of optical rectification and difference frequency generation (synchronous pumping of Cr^{2+}:II-VI oscillator by fs 1.5 μm fiber laser is very appealing in latter case).

It is important to mention that post-grown doping technology allows control (to some extent) of the TM:II-VI laser gain media microstructure (e.g., the average size of the grain). This allows tailoring the parameters of the gain element in favor of a certain type of three-wave mixing processes. Rigorous models of three-wave mixing in the randomly patterned polycrystalline TM:II-VI media should be developed to facilitate the optimization and fabrication of such tailored laser gain elements. Previous studies of patterned nonlinear materials show that properties of the material could be significantly altered due to the concentration of defects and mechanical stress at the domain boundaries [70].

Important directions for further research include power scaling of ultra-fast Cr^{2+}:II-VI lasers and extension of ultra-fast laser oscillations to 4–8 μm range.

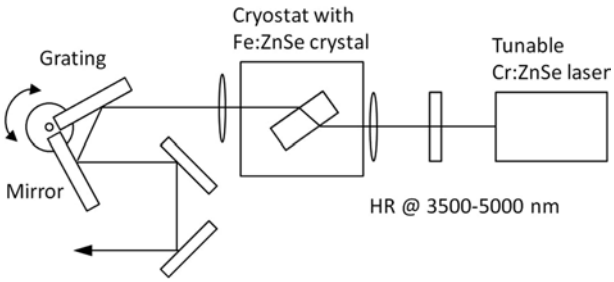

Fig. 25. A schematic of tunable CW Fe:ZnSe laser.

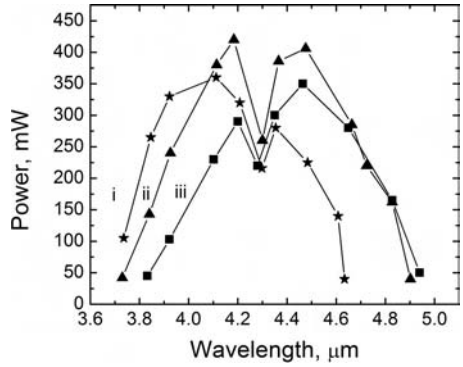

Fig. 26. Tuning curves of CW Fe:ZnSe laser at different temperatures: (i) 77 °K, (ii) 140 °K, and (iii) 170 °K.

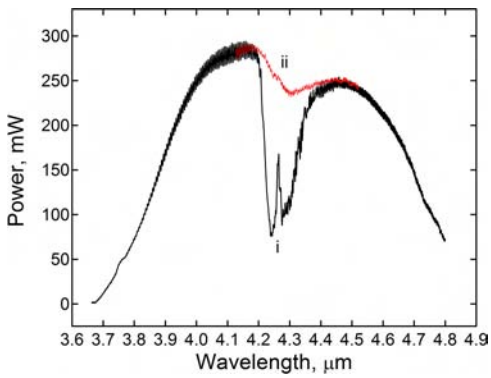

Fig. 27. Tuning curves of CW Fe:ZnSe laser at 140 °K (i) in ambient atmosphere, (ii) after 1 h purging with Ar.

Our preliminary experiments on amplification of the high repetition rate fs pulse train in cw pumped polycrystalline Cr^{2+}:ZnS laser amplifier [63] allow us to expect up to 5 W average output power in fs laser MOPA consisting of KLM master oscillator and robust cw pumped power amplifier.

Availability of reliable high power laser sources at 2–3 μm is a good starting point for the development ultra-fast 4–8 μm lasers. Such systems can be based on synchronously pumped OPO architecture [71], synchronously pumped Fe^{2+}:II-VI lasers or the Kerr-lens mode-locking of cw pumped Fe^{2+}:II-VI lasers.

IV. Fe:ZnSe/S Lasers

A. CW Fe:ZnSe/S Lasers

One of the major obstacles in developing CW Fe:ZnSe laser systems was a lack of available high power CW pump sources operating over 2.6–3.1 μm spectral range. 200 mW of output power from Fe:ZnSe single crystal laser was demonstrated in [49] at 77 K under 0.6 W 2.97 μm Cr:CdSe laser pumping. The output power of polycrystalline Fe:ZnSe was further scaled up to 840 mW in [72] at 77 K under 2.94 μm excitation with the radiation of two Sheaumann Laser MIR-PAC microchip lasers with a total pump power of 3 W. Recent progress in high power CW Cr:ZnSe lasers enabled utilization of these lasers as effective pump sources for Fe:ZnSe lasers. The detailed description of tunable CW Cr:ZnSe laser is given in Section III of this paper. The pump laser for the CW Fe:ZnSe laser presented below was a Cr:ZnSe laser tunable over 2.6–2.9 μm spectral range with 5.5 W output power. A schematic diagram of tunable CW Fe:ZnSe laser is depicted in Fig. 25. The laser cavity consists of a simple linear optical resonator formed by a plane high reflector, two lenses and diffraction grating operating in auto-collimation regime (Littrow mounting). The Fe:ZnSe crystal was placed at Brewster angle in liquid nitrogen cryostat with a temperature control.

We have found that varying the Fe:ZnSe gain element temperature over 77–170 °K allows tunability over 3700–4950 nm spectral range, as shown in Fig. 26. We also found that the optimal temperature of the gain element for the largest tuning range and output power is about 140 °K.

Fig. 27 shows a typical tuning curve of narrowline (<0.8 nm) Fe:ZnSe laser operating at 140 °K with additional intra-cavity aperture enabling TEM_{00} mode with M^2 <1.1.

A wide dip over 4.2–4.4 μm spectral range is due to intracavity absorption by atmospheric CO_2 and can be mitigated by cavity purging with Ar or N_2. The tuning upper limit of 4.8 μm was due to mechanical limitations of the tuning mechanism. It is noteworthy that by replacing the diffraction grating with 70% output coupler we obtained, 1.6 W of output power at 4.1 μm in a non-selective cavity. The efficiency of lasing with regards to the pump power was 30%. There was no indication of thermal rollover and Fe:ZnSe output power was limited by the power of available pump source. To the best of our knowledge, it is the highest output power reported for cw Fe:ZnSe lasers.

B. Gain-Switched Fe:ZnS and Fe:ZnSe Lasers

Direct quasi-resonant pumping of Q-switched Ho:YAG lasers by Tm-fiber lasers operating at 1908 nm allows for obtaining high energy nanosecond pulsed output radiation at 2.09 μm at pulse repetition rates ranging from tens of Hz to hundreds of kHz with high optical to optical efficiencies. The Ho:YAG lasers find numerous potential applications as laser processing tools in material processing fields where nanosecond pulsed laser radiation is required for efficient ablation processes of tough materials. Another very important application of fiber-pumped Q-switched Ho:YAG lasers is pumping of Cr:ZnSe gain crystals in gain-switched laser configuration. This approach allows for obtaining 2–5 ns pulses in the spectral range of 2–3 μm. The latter system can be used as standalone laser processing tool for variety of applications in material processing and as

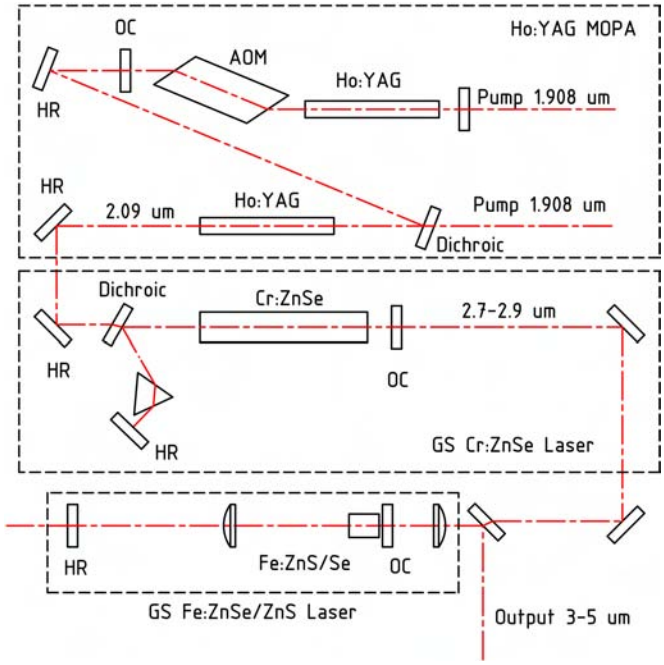

Fig. 28. Optical scheme of Fe^{2+}:ZnS/ZnSe laser systems. The Tm-fiber laser pumped Ho:YAG MOPA system is used to pump gain-switched Cr^{2+}:ZnSe tunable laser, which is used as a pulsed nanosecond source to pump the Fe^{2+}:ZnS or Fe^{2+}:ZnSe gain media.

an efficient pump source for Fe:ZnS and Fe:ZnSe mid-IR gain media to obtain short nanosecond pulses in the spectral range of 3–5 μm, which is of high interest for scientific, medical, industrial, environmental, and defense related applications.

The most general optical scheme of our gain switched Fe^{2+}:ZnS and Fe^{2+}:ZnSe laser is shown in Fig. 28.

The Ho:YAG MOPA is resonantly pumped by high-power Tm fiber laser and is actively Q-switch by an AOM and serves as the pump source for tunable Cr^{2+}:ZnSe module. The output wavelength of the gain-switched Cr^{2+}:ZnSe laser is tuned close to the absorption peak of Fe^{2+}:ZnS or Fe^{2+}:ZnSe gain media (within 2.7–2.9 μm spectral range). The Fe^{2+}:ZnS/ZnSe is based on a simple stable resonator for advanced control of the output beam quality and is pumped through a dichroic output coupler. The input-output characteristics of this mid-IR laser cascade operating near 1 kHz pulse rate are shown in Fig. 29. The output spectra of gain-switched Fe^{2+}:ZnS and Fe^{2+}:ZnSe lasers are shown in Fig. 30. All the results of gain-switched operation of Fe:ZnS/ZnSe lasers were demonstrated at RT. RT lasing is possible when the pump pulse duration is shorter or of the order of magnitude of the Fe:ZnS/ZnSe RT lifetime (several hundred nanoseconds).

The output energy of Fe^{2+}:ZnS/Se lasers in these experiments was limited mainly by optical damage thresholds of the gain crystals. We are currently working on further improvements of the laser design to obtain multi-mJ output energies in the 3–5 μm spectral range. Table III summarizes the output parameters of the gain-switched Fe^{2+}:ZnS/ZnSe laser systems.

Recently the output energy of the gain switched Fe:ZnSe laser was scaled up to 30 mJ at 125 ns pulses at RT [40] with the use

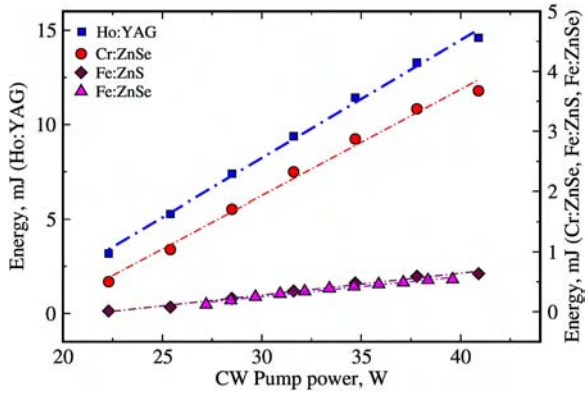

Fig. 29. Input-output characteristics of the multi-cascade Fe^{2+}:ZnS/ZnSe laser. Left *y*-axis shows performance of the Ho:YAG module, right *y*-axis shows corresponding output energies of the gain-switched Cr^{2+}:ZnSe, Fe^{2+}:ZnS, and Fe^{2+}:ZnSe modules.

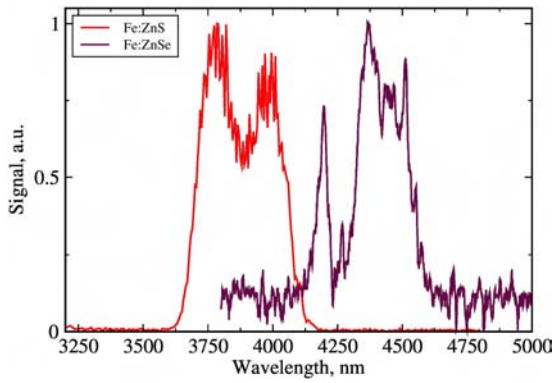

Fig. 30. Output spectra of gain-switched Fe^{2+}:ZnS and Fe^{2+}:ZnSe lasers. The laser mirrors have broadband reflectivity profile and no spectral control is performed, resulting in broad linewidth located near the maximum gain.

TABLE III
SUMMARY OF THE OUTPUT CHARTERISTICS OF THE GAIN-SWITCHED Fe^{2+}:ZNS/ZNSE LASER SYSTEMS

Gain medium	R, KHz	E_{out}, mJ	λ, μm	τ, ns
Fe:ZnS	0.9	0.6	3.98	7
Fe:ZnSe	0.7	0.53	4.36	12
Fe:ZnSe	1.0	0.33	4.36	12

R– pulse repetition rate, E_{out} – output energy, λ - output wavelength, τ pulse duration.

of non-chain electric discharge HF laser and further increase of the output energy was demonstrated to be feasible.

C. Free Running Fe:ZnSe Lasers

The flash-lamp pumped, free-running Er:YAG (Er:YSGG) lasers operating at 2.94 μm (2.78 μm) are excellent pump sources for applications which require high energy pulses rather than high repetition rate. The authors of [73] reported utilization of a flashlamp pumped Er:YAG laser (oscillation wavelength 2.94 μm and 250 μs pulse duration) for development of a high energy Fe:ZnSe laser. The maximum used repetition rate of the

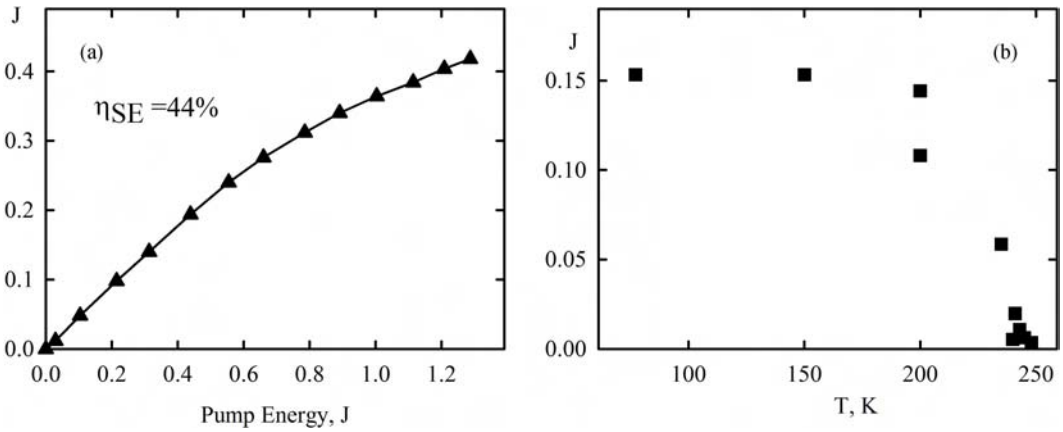

Fig. 31. (a) Output energy at 4.16 μm of the Fe:ZnSe laser versus pump energy measured at 77 K. (b) Temperature dependence of the output energy of the Fe:ZnSe laser.

TABLE IV
STATE-OF-THE-ART IN CR:ZNSE/S AND FE:ZNSE/S LASERS

Gain element	WAVELENGTH, μM	LINE WIDTH	W, Av.	W, Peak	Rep Rate	Pulse Energy	τ_p	Eff.,%	Type	T	Pump	Ref.
Cr:ZnS/ ZnSe lasers												
Cr:ZnS	2.3	1 nm	0.5 W					40%	CW	RT	Diode	[50]
Cr:ZnSe	2.4	$<$0.5 nm	3.7 W					12%	CW	RT	Diode@1.7 μm	[74]
Cr:ZnSe	2.4	1 nm	30 W					50%	CW	RT	Tm-fiber@1.9 μm	[*]
Cr:ZnSe	2.3	$<$0.7 kHz	5.5 W						CW	RT	Tm-fiber@1.9 μm	[*]
Cr:ZnSe	2.3	100 kHz	160 mW					12%	CW	RT	Diode/Er-fiber @1.56 um	[14]
Cr:ZnSe	2.94	1 nm	10 W					25%	CW	RT	Tm-fiber@1.9 μm	[*]
Cr:ZnS	2.3	82 nm	2 W	275 kW	94.5 MHz	21 nJ	67 fs	20%	ML	RT	Er-fiber@1.56 μm	[*]
Cr:ZnS	2.3	120 nm	0.6 W	140 kW	94.5 MHz	7 nJ	$<$46 fs	12%	ML	RT	Er-fiber@1.56 μm	[*]
Cr:ZnSe	2.475	37 nm	0.35 W	1 GW	1 kHz	0.35 mJ	346 fs		ML^m	RT	Tm-fiber@1.9 μm	[26]
Cr:ZnSe	2.45		18.5 W	26 kW	7 kHz	2.64 mJ	125 ns	56%	GS	RT	Tm:YAP@1.94 μm	[75]
Cr:ZnSe	2.35	2 GHz	5.5 W	8.8 kW	5 kHz	1.1 mJ	125 ns		GS^m	RT	Tm:YAP@1.94 μm	[75]
Cr:ZnSe	2.4	150 nm	200 mW	2 MW	10 Hz	20 mJ	10 ns	30%	GS	RT	Raman Laser @1.9μm	[58]
Cr:ZnSe	2.43		500 mW	0.33 MW	10 Hz	50 mJ	150 ns	4.5%	GS^m	RT	Tm-fiber@1.9 μm	[59]
Cr:ZnSe	2.65	50 nm	110 mW	160 W	0.1 Hz	1.1 J	7 ms	15%	FR	RT	Er:Glass@1.54 μm	[60]
Fe:ZnS/ZnSe lasers												
Fe:ZnSe	4.1	50 nm	1.6 W					30%	CW	77 K	Cr:ZnSe@2.7μm	[*]
Fe:ZnSe	4.065	40 nm	515 mW	8.3 W	850 kHz	0.6μJ	64 ns	22%	QS	77 K	Er:YAG@2.9 μm	[76]
Fe:ZnSe	4.0	20 nm	1 W	0.2 MW	1 kHz	1	5 ns	30%	GS	RT	Cr:ZnSe@2.7μm	[*]
Fe:ZnS	3.95	300 nm	0.5 W	0.15 MW	0.7 kHz	0.7 mJ	5 ns	25%	GS	RT	Cr:ZnSe@2.7μm	[*]
Fe:ZnS	3.85	200 nm		68 kW		3.4 mJ	50 ns	32%	GS	RT	Er:YAG@2.9μm	[77]
Fe:ZnSe	4.1	30 nm		0.25 MW	5 Hz	5 mJ	20 ns	19%	GS	RT	Er:YSGG@2.8 μm	[39]
Fe:ZnSe	4.1		0.6 W	0.24 MW	20 Hz	30 mJ	125 ns	3–5%	GS	RT	HF@3 μm	[40]
Fe:ZnSe	4.1	20 nm	2.5 W	1.6 kW	5 Hz	0.4 J	250 μs	32%	FR	77 K	Er:YAG@2.9μm	[43]
Fe:ZnSe	4.1			2.8 kW		2.1 J	750 μs	25%	FR	77 K	Er:YAG@2.9μm	[44]
Fe:ZnSe	4.1					42 mJ	750 μs	1%	FR	RT	Er:YAG@2.9μm	[44]

Wavelength is central oscillation wavelength for tunable lasers; Lasers regimes of oscillation: CW-continues wave; ML- mode-locked; QS- Q-switched; GS-gain-switched; FR- long pulse (free running); superscript "m"- MOPA configuration; [$*$] -current paper).

pump laser was 11 Hz. The maximum pump energy of non-polarized radiation was 1.5 J. Typical pulse duration of the Er free-running lasers is usually within 200–300 μs pulse duration. It is significantly longer than Fe-ion upper-level life-time at RT ($\sim$300 ns). Therefore, an efficient operation of Fe:ZnSe lasers under free-running excitation requires cooling of the gain elements. The Fe:ZnSe gain element was mounted at Brewster angle to the cavity axis in the liquid nitrogen cryostat. The best results were obtained in the flat-flat cavity with a 70% output coupler reflectivity. The laser output–input dependence with respect to the pump energy at 77 K is depicted in Fig. 31(a). The laser slope efficiency of 44% was realized for pump energy

below 0.5 J. The output–input characteristics of the Fe:ZnSe laser were studied at different temperatures ranging from 77 K to 250 K. Fe:ZnSe output energy up to 0.5 J has been demonstrated with a real optical efficiency of 32% with respect to pump energy. The temperature dependence of the output energy is shown in Fig. 31(b). The laser oscillation was demonstrated for temperatures below 250 K. For the compact systems, this temperature could be achieved by using thermo-electric coolers. The laser linewidth in the nonselective laser cavity was measured to be 60 nm at 77 K. The laser oscillation was tuned with temperature from 4.16 to 4.65 μm for 77 K–250 K temperature range. The laser cavity with CaF_2 prism allowed us to obtain tunable oscillation between 3.9 and 5.1 μm spectral range with oscillation linewidth $<$3 nm.

In a recent publication [41] the output energy of free-running Fe:ZnSe laser was further scaled up to 2.1 J at 85 K under 8 J pump radiation of a long pulse (750 μs) Er:YAG laser. By operating at 245 K (temperature reachable by thermo-electric coolers) a 1.3 J of output energy was achieved at 23% optical-to-optical efficiency. For the first time room temperature operation was achieved for free-running regime of Fe:ZnSe lasing. The maximum energy reached 42 mJ at RT with efficiency of $\sim$1%.

The output characteristics of free-running Fe:ZnSe laser systems show the possibility of developing effective multi-joule sources in 3.5–5 μm spectral range.

V. Summary and Outlook

Chromium and iron doped ZnSe and ZnS lasers have come of age, and, arguably, represent nowadays the most effective route for lasing over 1.9–5 um spectral range with multi-watt average power, peak power up to 1 GW, multi-Joule energy and pulse durations as short as 40 fs. A summary of the state-of-the-art Cr and Fe doped ZnSe and ZnS lasers is provided in Table IV.

Future progress of Cr- and Fe-doped II-VI lasers in terms of extending spectral coverage over 3–4 μm and 5–6 μm depends on a search of new, low-phonon-cutoff Cr- and Fe-doped binary and ternary II-VI semiconductors bulk materials. Future improvements in output power will depend on new schemes of thermal management of gain elements including utilization of fiber, waveguide and disk geometry. Future improvements in technology of hot-pressed ceramic II-VI compounds can stimulate design flexibility of the laser elements with high optical quality (undoped ends, gradient of dopant concentration, etc) important for development of efficient, high performance lasers with output power and energy scaled-up to hundreds of Watts and several Joules.

Acknowledgment

The authors are grateful to their colleagues and collaborators: V. Gapontsev, F. Stukalin, T. Ness, M. O'Connor, N. Platonov, T. King, Y. Kateshov, A. Zakrevskiy, S. Klyuyev, K. Schepler, P. Berry, J. Goldstein, I. Sorokina, E. Sorokin, S. Trivedi, J. Williams, R. Camata, K. Graham, A. Gallian, C. Kim, N. Myoung, Y. Terekhov, T. Konak, J. Peppers, and A. Martinez. The work reported here partially involves intellectual property developed at the University of Alabama at Birmingham (UAB). This intellectual property has been licensed to the IPG Photonics Corporation. The UAB co-authors declare competing financial interests.

References

[1] L. D. DeLoach, R. H. Page, G. D. Wilke, S. A. Payne, and W. F. Krupke, "Transition metal-doped zinc chalcogenides: Spectroscopy and laser demonstration of a new class of gain media," *IEEE J. Quantum Electron.*, vol. 32, no. 6, pp. 885–895, Jun. 1996.

[2] R. H. Page, K. I. Shaffers, L. D. DeLoach, G. D. Wilke, F. D. Patel, J. B. Tassano, S. A. Payne, W. F. Krupke, K. T. Chen, and A. Burger, "Cr^{2+}-doped sinc chalcogenides as efficient, widely tunable mid-infrared lasers," *IEEE J. Quantum Electron.*, vol. 33, no. 4, pp. 609–619, Apr. 1997.

[3] R. H. Page, J. A. Skidmore, K. I. Schaffers, R. J. Beach, S. A. Payne, and W. F. Krupke, "Demonstrations of diode-pumped and grating tuned ZnSe:Cr^{2+} lasers," *OSA Trends Opt. Photon.*, vol. 10, pp. 208–210, 1997.

[4] E. Sorokin, I. T. Sorokina, and R. H. Page, "Room-temperature CW diode-pumped Cr^{2+}:ZnSe laser," *OSA Trends Opt. Photon.*, vol. 46, pp. 101–105, 2001.

[5] M. Mond, E. Heumann, G. Huber, H. Kretschmann, S. Kuck, A. V. Podlipensky, V. G. Shcherbitsky, N. V. Kuleshov, V. I. Levchenko, and V. N. Yakimovich, "Continuous-wave diode pumped Cr^{2+}:ZnSe and high power laser operation," *OSA Trends Opt. Photon.*, vol. 46, pp. 162–165, 2001.

[6] G. J. Wagner, T. J. Carrig, R. H. Page, K. I. Schaffers, J. Ndap, X. Ma, and A. Burger, "Continuous-wave broadly tunable Cr^{2+}:ZnSe laser," *Opt. Lett.*, vol. 24, pp. 19–21, 1999.

[7] T. J. Carrig, G. J. Wagner, W. J. Alford, and A. Zakel, "Chromium-doped chalcogenides lasers," *Proc. SPIE*, vol. 5460, pp. 74–82, 2004.

[8] U. Demirbas and A. Sennaroglu, "Intracavity-pumped Cr^{2+}:ZnSe laser with ultrabroadband tuning range between 1880 and 3100 nm," *Opt. Lett.*, vol. 31, pp. 2293–2295, 2006.

[9] S. B. Mirov, V. V. Fedorov, K. Graham, I. Moskalev, V. Badikov, and V. Panyutin, "Er-fiber laser pumped continuous-wave microchip Cr^{2+}:ZnS and Cr^{2+}:ZnSe lasers," *Opt. Lett.*, vol. 27, pp. 909–911, 2002.

[10] S. B. Mirov, V. V. Fedorov, K. Graham, I. S. Moskalev, I. T. Sorokina, E. Sorokin, V Gapontsev, D. Gapontsev, V. V. Badikov, and V. Panyutin, "Diode and fiber pumped Cr^{2+}:ZnS mid-IR external cavity and microchip lasers," *IEE Optoelectronics*, vol. 150, no. 4, pp. 340–345, 2003.

[11] K. L. Schepler, R. D. Peterson, P. A. Berry, and J. B. McCay, "Thermal effects in Cr^{2+}:ZnSe thin disk laser," *IEEE J. Quantum Electron.*, vol. 11, no. 3, pp. 713–720, May/Jun. 2005.

[12] G. J. Wagner, B. G. Tiemann, W. J. Alford, and T. J. Carrig, "Single-frequency Cr:ZnSe laser," presented at the Adv. Solid-State Photon., Washington, DC, USA, 2004, Paper WB12.

[13] I. S. Moskalev, V. V. Fedorov, and S. B. Mirov, "Tunable, single-frequency, and multi-watt continuous-wave Cr^{2+}:ZnSe lasers," *Opt. Exp.*, vol. 16, no. 6, pp. 4145–4153, 2008.

[14] N. Coluccelli, M. Cassinerio, P. Laporta, and G. Galzerano, "100 kHz linewidth Cr^{2+}:ZnSe ring laser tunable from 2.12 to 2.58 μm," *Opt. Lett.*, vol. 37, no. 24, pp. 5088–5090, 2012.

[15] I. T. Sorokina, "Cr^{2+}-doped II–VI materials for lasers and nonlinear optics," *Opt. Mater.*, vol. 26, pp. 395–412, 2004.

[16] C. Kim, D. V. Martyshkin, V. V. Fedorov, and S. B. Mirov, "Mid-infrared Cr^{2+}:ZnSe random powder lasers," *Opt. Exp.*, vol. 16, no. 7, pp. 4952–4959, 2008.

[17] C. Kim, D. V. Martyshkin, V. V. Fedorov, and S. B. Mirov, "Middle-infrared random lasing of Cr^{2+} doped ZnSe, ZnS, CdSe powders, powders imbedded in polymer liquid solutions, and polymer films," *Opt. Commun.*, vol. 282, pp. 2049–2052, 2009.

[18] I. S. Moskalev, S. B. Mirov, and V. V. Fedorov, "Multiwavelength mid-IR spatially-dispersive CW laser based on polycrystalline Cr^{2+}:ZnSe," *Opt. Exp.*, vol. 12, pp. 4986–4992, 2004.

[19] V. V. Fedorov, A. Gallian, I. Moskalev, and S. B. Mirov, "En route to electrically pumped broadly tunable middle infrared lasers based on transition metal doped II-VI semiconductors," *J. Luminescence*, vol. 125, pp. 184–195, 2007.

[20] A. Gallian, V. V. Fedorov, S. B. Mirov, V. V. Badikov, S. N. Galkin, E. F. Voronkin, and A. I. Lalayants, "Hot-pressed ceramic Cr^{2+}:ZnSe gain-switched laser," *Opt. Exp.*, vol. 14, pp. 11694–11701, 2006.

[21] T. J. Carrig, G. J. Wagner, A. Sennaroglu, J. Y. Jeong, and C. R. Pollock, "Mode-locked Cr^{2+}:ZnSe laser," *Opt. Lett.*, vol. 25, pp. 168–170, 2000.

[22] I. Sorokina, E. Sorokin, A. Di Lieto, M. Tonelli, R. H. Page, and K. I. Schaff, "Active and passive mode-locking of Cr^{2+}:ZnSe laser," presented at the Advanced Solid-State Lasers, Seattle, WA, USA, 2001, Paper MC2

[23] C. Pollock, N. Brilliant, D. Gwin, T. J. Carrig, W. J. Alford, J. B. Heroux, W. I. Wang, I. Vurgaftman, and J. R. Meyer, "Mode locked and Q-switched Cr:ZnSe laser using a semiconductor saturable absorbing mirror (SESAM)," presented at the Adv Solid-State Photon., Vienna, Austria, 2005, Paper TuA6.

[24] I. T. Sorokina, E. Sorokin, and T. Carrig, "Femtosecond pulse generation from a SESAM mode-locked Cr:ZnSe laser," presented at the Conf. Lasers Electro-Opt., Long Beach, CA, USA, 2006, Paper CMQ2.

[25] M. N. Cizmeciyan, H. Cankaya, A. Kurt, and A. Sennaroglu, "Kerr-lens mode-locked femtosecond Cr^{2+}:ZnSe laser at 2420 nm," *Opt. Lett.*, vol. 34, pp. 3056–3058, 2009.

[26] P. Moulton and E. Slobodchikov, "1-GW-peak-power, Cr:ZnSe laser," presented at the CLEO: Appl. Technol., Baltimore, MD, USA, 2011, Paper PDPA10.

[27] I. S. Moskalev, V. V. Fedorov, and S. B. Mirov, "10-Watt, room-temperature, pure continuous-wave, polycrystalline Cr^{2+}:ZnS laser," *Opt. Exp.*, vol. 17, no. 4, pp. 2048–2056, 2009.

[28] I. T. Sorokina, E. Sorokin, S. B. Mirov, V. V. Fedorov, V. Badikov, V. Panyutin, and K. Schaffers, "Broadly tunable compact continuous-wave Cr^{2+}:ZnS laser," *Opt. Lett.*, vol. 27, pp. 1040–1042, 2002.

[29] I. T. Sorokina, E. Sorokin, T. J. Carrig, and K. I. Schaffers, "A SESAM passively mode-locked Cr:ZnS laser," presented at the Adv. Solid State Photon., Incline Village, NV, USA, 2006, Paper TuA4.

[30] N. Tolstik, E. Sorokin, and I. T. Sorokina, "Kerr-lens mode-locked Cr:ZnS laser," *Opt. Lett.*, vol. 38, pp. 299–301, 2013.

[31] E. Sorokin, N. Tolstik, and I. T. Sorokina, "1 Watt femtosecond mid-IR Cr:ZnS laser," in *Proc. SPIE*, vol. 8599, pp. 859916-1-859916–7, 2013.

[32] N. Tolstik, E. Sorokin, and I. T. Sorokina, "Graphene mode-locked Cr:ZnS laser with 41 fs pulse duration," *Opt. Exp.*, vol. 22, pp. 5564–5571, 2014.

[33] U. Hommerich, X. Wu, V. R. Davis, S. B. Trivedi, K. Grasze, R. J. Chen, and S. W. Kutcher, "Demonstration of room temperature laser action at 2.5 μm from Cr^{2+}:$Cd_{0.85}Mn_{0.15}Te$," *Opt. Lett.*, vol. 22, pp. 1180–1182, 1997.

[34] J. McKay, K. L. Schepler, and G. C. Catella, "Efficient grating–tuned mid-infrared Cr^{2+}:CdSe laser," *Opt. Lett.*, vol. 24, pp. 1575–1577, 1999.

[35] V. A. Akimov, V. I. Kozlovsky, Y. V. Korostelin, A. I. Landman, Y. P. Podmar'kov, Y. K. Skasyrsky, and M. P. Frolov, "Efficient cw lasing in a Cr^{2+}:CdSe crystal," *Quantum Electron.*, vol. 37, no. 11, pp. 991–992, 2007.

[36] V. A. Akimov, V. I. Kozlovsky, Y. V. Korostelin, A. I. Landman, Y. P. Podmar'kov, Y. K. Skasyrsky, and M. P. Frolov, "Efficient pulsed Cr^{2+}CdSe laser continuously tunable in the spectral range from 2.26 to 3.61 μm," *Quantum Electron.*, vol. 38, no. 3, pp. 205–208, 2008.

[37] J. J. Adams, C. Bibeau, R. H. Page, D. M. Krol, L. H. Furu, and S. A. Payne, "4.0–4.5 μm lasing of Fe:ZnSe below 180 K, a new mid-infrared laser material," *Opt. Lett.*, vol. 24, pp. 1720–1722, 1999.

[38] J. Kernal, V. V. Fedorov, A. Gallian, S. B. Mirov, and V. Badikov, "3.9–4.8 μm gain-switched lasing of Fe:ZnSe at room temperature," *Opt. Exp.*, vol. 13, no. 26, pp. 10608–10615, 2005.

[39] N. Myoung, D. V. Martyshkin, V. V. Fedorov, and S. B. Mirov, "Energy scaling of 4.3 μm room temperature Fe:ZnSe laser," *Opt. Lett.*, vol. 36, no. 1, pp. 94–96, 2011.

[40] S. D. Velikanov, V. P. Danilov, N. G. Zakharov, N. N. Il'ichev, S. Yu. Kazantsev, V. P. Kalinushkin, I. G. Kononov, A. S. Nasibov, M. I. Studenikin, P. P. Pashinin, K. N. Firsov, P. V. Shapkin, and V. V. Shchurov, "Fe^{2+}:ZnSe laser pumped by a nonchain electric-discharge HF laser at room temperature," *Quantum Electron.*, vol. 44, no. 2, pp. 141–144, 2014.

[41] A. A. Voronov, V. I. Kozlovskii, Y. V. Korostelin, A. I. Landman, Y. P. Podmar'kov, and M. P. Frolov, "Laser parameters of a Fe:ZnSe laser crystal in the 85–255K temperature range," *Quantum Electron.*, vol. 35, no. 9, pp. 809–812, 2005.

[42] V. V. Fedorov, S. B. Mirov, A. Gallian, D. V. Badikov, M. P. Frolov, Y. V. Korostelin, V. I. Kozlovsky, A. I. Landman, Y. P. Podmar'kov, V. A. Akimov, and A. A. Voronov, "3.77–5.05-μm tunable solid state lasers based on Fe^{2+}-doped ZnSe crystals operating at low and room temperatures," *IEEE J. Quantum Electron.*, vol. 42, no. 9, pp. 907–917, Sep. 2006.

[43] V. Fedorov, D. Martyshkin, M. Mirov, I. Moskalev, S. Vasilyev, J. Peppers, V. Gapontsev, and S. Mirov, "Fe-doped binary and ternary II-VI mid-infrared laser materials," presented at the Adv. Solid-State Lasers, Paris, France, 2013, Paper AW1A.8.

[44] M. P. Frolov, Y. V. Korostelin, V. I. Kozlovsky, V. V. Mislavskii, Y. P. Podmar'kov, S. A. Savinova, and Y. K. Skasyrsky, "Study of a 2-J pulsed Fe:ZnSe 4-μm laser," *Laser Phys. Lett.*, vol. 10, pp. 125001–125007, 2013.

[45] I. T. Sorokina, "Crystalline Mid-Infrared lasers," in *Proc. SPIE*, vol. 79,, pp. 255–350, 2003.

[46] E. Sorokin, S. Naumov, and I. T. Sorokina, "Ultrabroadband infared solid state lasers," *IEEE J. Sel. Topics Quantum Electron.*, vol. 11, no. 3, pp. 690–712, May/Jun. 2005.

[47] S. Mirov, V. Fedorov, I. Moskalev, and D. Martyshkin, "Recent progress in transition metal doped II-VI mid-IR lasers," *IEEE J. Sel. Topics Quantum Electron.*, vol. 13, no. 3, pp. 810–822, May/Jun. 2007.

[48] A. Sennaroglu and U. Demibras, "Tunable Cr^{2+}:ZnSe lasers in the mid-infrared," in *Solid State Lasers and Applications*, A. Sennaroglu, Ed. Boca Raton, FL, USA: CRC Press, 2007, pp. 113–162.

[49] V. I. Kozlovsky, V. A. Akimov, M. P. Frolov, Y. V. Korestelin, A. I. Landman, V. P. Martovitsky, V. V. Mislavskii, Y. P. Podmar'kov, Y. K. Skasyrsky, and A. A. Voronov, "Room-temperature tunable mid-infrared lasers on transition-metal doped II-VI compound crystals grown from vapor phase," *Phys. Status Solidi(b)*, vol. 247, no. 6, pp. 1553–1556, 2010.

[50] S. B. Mirov, V. V. Fedorov, I. S. Moskalev, D. Martyshkin, and C. Kim, "Progress in Cr^{2+} and Fe^{2+} doped mid-ir laser materials," *Laser Photon. Rev.*, vol. 4, no. 1, pp. 21–41, 2010.

[51] S. B. Mirov, V. V. Fedorov, D. V. Martyshkin, I. S. Moskalev, M. S. Mirov, and V. P. Gapontsev, "Progress in Mid-IR Cr^{2+} and Fe^{2+} doped II-VI materials and lasers," *Opt. Mat. Exp.*, vol. 1, pp. 898–910, 2011.

[52] S. Mirov, V. Fedorov, I. Moskalev, M. Mirov, and D. Martyshkin, "Frontiers of mid-infrared lasers based on transition metal doped II–VI semiconductors," *J. Lumin.*, vol. 133, pp. 268–275, 2013.

[53] W. F. Krupke, "Induced emission cross-sections in neodymium laser glasses," *IEEE J. Quantum Electron.*, vol. 10, no. 4, pp. 450–457, Apr. 1974.

[54] G. A. Slack, F. S. Ham, and R. M. Chrenko, "Optical absorption of tetrahedral Fe^{2+} (3d6) in cubic ZnS, CdTe, and $MgAl_2O_4$," *Phys. Rev.*, vol. 152, pp. 376–402, 1966.

[55] N. Myoung, V. V. Fedorov, S. B. Mirov, and L. E. Wenger, "Temperature and concentration quenching of mid-IR photoluminescence in iron doped ZnSe and ZnS laser crystals," *J. Lumin.*, vol. 132, no. 3, pp. 600–606, 2012.

[56] G. Goetz and H.-J. Schulz, "Decay of internal luminescence transitions of 3d impurities in II–VI compounds. Recent experiments and refined interpretations," *J. Lumin.*, vol. 40–41, pp. 415–416, 1988.

[57] L. Podlowski, R. Heitz, P. Thurian, A. Hoffmann, and I. Broser, "Non-radiative transition rates of Fe^{2+} in III–V and II–VI semiconductors," *J. Lumin.*, vol. 58, pp. 252–256, 1994.

[58] V. V. Fedorov, I. S. Moskalev, M. S. Mirov, S. B. Mirov, T. J. Wagner, M. J. Bohn, P. A. Berry, and K. L. Schepler, "Energy scaling of nanosecond gain-switched Cr^{2+}:ZnSe lasers," *Proc. SPIE*, vol. 7912, Paper 79121E, 2011.

[59] N. Saito, M. Yumoto, T. Tomida, U. Takagi, and S. Wada, "All-solid-state rapidly tunable coherent 6–10 μm light source for lidar environmental sensing," *Proc. SPIE*, vol. 8526, Paper 852605, 2012.

[60] V. Fedorov, M. S. Mirov, S. Mirov, V. Gapontsev, A. V. Erofeev, M. Z. Smirnov, and G. B. Altshuler, "Compact 1J mid-IR Cr:ZnSe Laser," presented at the *Frontiers Opt.*, Rochester, New York, USA, 2012, Paper FW6B.9.

[61] M. N. Cizmeciyan, H. Cankaya, A. Kurt, and A. Sennaroglu, "Operation of femtosecond Kerr-lens mode-locked Cr:ZnSe lasers with different dispersion compensation methods," *Appl. Phys. B*, vol. 106, pp. 887–892, 2012.

[62] E. Sorokin, N. Tolstik, K. I. Schaffers, and I. T. Sorokina, "Femtosecond SESAM-modelocked Cr:ZnS laser," *Opt. Exp.*, vol. 20, pp. 28947–28952, 2012.

[63] S. Vasilyev, M. Mirov, and V. Gapontsev, "Kerr-lens mode-locked femtosecond polycrystalline Cr^{2+}:ZnS and Cr^{2+}:ZnSe lasers," *Opt. Exp.*, vol. 22, pp. 5118–5123, 2014.

[64] H. P. Wagner, M. Kühnelt, W. Langbein, and J. M. Hvam, "Dispersion of the second-order nonlinear susceptibility in ZnTe, ZnSe, and ZnS," *Phys. Rev. B*, vol. 58, p. 10494, 1998.

[65] B. E. Bouma and J. G. Fujimoto, "Compact Kerr-lens mode-locked resonators," *Opt. Lett.*, vol. 21, pp. 134–136, 1996.

[66] V. P. Gribkovsky, V. A. Zyulkov, A. E. Kazachenko, and V. A. Shakin, "Second harmonic generation on the grating of optical inhomogeneities in ZnSe and ZnS," *Phys. Stat. Solidi(b)*, vol. 159, p. 379, 1990.

[67] E. Yu. Morozov, A. A. Kaminskii, A. S. Chirkin, and D. B. Yusupov, "Second optical harmonic generation in nonlinear crystals with a disordered domain structure," *JETP Lett.*, vol. 73, pp. 647–650, 2001.
[68] M. Baudrier-Raybaut, R. Haïdar, P. Kupecek, P. Lemasson, and E. Rosencher, "Random quasi-phase-matching in bulk polycrystalline isotropic nonlinear materials," *Nature*, vol. 432, pp. 374–376, 2004.
[69] E. Sorokin and I. T. Sorokina, "Femtosecond operation and random quasi-phase-matched self-doubling of ceramic Cr:ZnSe Laser," presented at the Conf. Lasers Electro-Opt., San Jose, CA, USA, 2010, Paper CTuGG2.
[70] S. Vasilyev, H.-E. Gollnick, A. Nevsky, A. Grisard, E. Lallier, B. Gérard, J. Jimenez, and S. Schiller, "Counterdirectional mode coupling in ring resonators with QPM nonlinear crystals and effects on the characteristics of cw optical parametric oscillation," *Appl. Phys. B*, vol. 100, p. 737, 2010.
[71] K. L. Vodopyanov, E. Sorokin, I. T. Sorokina, and P. G. Schunemann, "Mid-IR frequency comb source spanning 4.4–5.4 μm based on subharmonic GaAs optical parametric oscillator," *Opt. Lett.*, vol. 36, pp. 2275–2277, 2011.
[72] J. W. Evans, P. A. Berry, and L. L. Schepler, " 840 mW continuous-wave Fe:ZnSe laser operating at 4140 nm," *Opt. Lett.*, vol. 37, no. 23, pp. 5021–5023, 2012.
[73] V. Fedorov, D. Martyshkin, M. Mirov, I. Moskalev, S. Vasilyev, J. Peppers, V. Gapontsev, and S. Mirov, "Fe-doped binary and ternary II-VI mid-infrared laser materials," presented at the Adv. Solid-State Lasers, Paris, France, 2013, Paper AW1A.8.
[74] G. J. Wagner, A. M. Schober, G. T. Bennett, D. L. Bruns, J. H. Marquardt, T. J. Carrig, "Multi-Watt broadly-tunable diode-pumped Cr:ZnSe laser," presented at the Lasers Electro-Opt., San Jose, CA, USA, pp. 1–2, May 6–11, 2012.
[75] A. Zakel, G. Wagner, A. Sullivan, J. Wenzel, W. Alford, and T. Carrig, "High-brightness, rapidly-tunable Cr:ZnSe lasers," presented at the Adv. Solid-State Photon., Vienna, Austria, 2005, Paper MD2.
[76] J. W. Evans, P. A. Berry, and K. L. Schepler, "A passively Q-switched, CW-pumped Fe:ZnSe Laser," *IEEE J. Quantum Electron.*, vol. 50, no. 3, pp. 204–209, Mar. 2014.
[77] V. I. Kozlovsky, Y. V. Korostelin, A. I. Landman, V. V. Mislavskii, Y. P. Podmar'kov, Y. K. Skasyrsky, and M. P. Frolov, "Pulsed Fe^{2+}:ZnS laser continuously tunable in the wavelength range of 3.49- 4.65 μm," *Quantum Electron.*, vol. 41, no. 1, pp. 1–3, 2011.

Sergey B. Mirov was born in Moscow, Russia, in 1955. He received the M.S. degree in electronic engineering from the Moscow Power Engineering Institute—Technical University, Moscow, Russia, in 1978, and the Ph.D. degree in physics from the P. N Lebedev Physics Institute of the Russian Academy of Sciences, Moscow, in 1983 for his work on tunable color center lasers. He served as a Staff Research Physicist at P. N. Lebedev Physics Institute, and a Principal Research Scientist and a Group Leader at the General Physics Institute of the Russian Academy of Sciences. His early work in Russian Academy of Sciences involved physics of color centers formation under ionizing irradiation, color center's photo chemistry, laser spectroscopy of solids and led to the development of the first room temperature operable commercial color center lasers, passive Q-switches and nonlinear filters for various types of neodymium lasers from mini lasers to powerful laser glass systems. He received the USSR First National Prize for Young Scientists, in 1982, for the development of LiF color center saturable absorbers. He received Distinguished Research Award from the General Physics Institute, in 1985 and 1989, and from the P N. Lebedev Physical Institute in 1980. Since 1993, he is a faculty member at the Department of Physics, University of Alabama at Birmingham (UAB), USA. He is currently a University Professor of physics at the UAB, the Director of the Center for Optical Sensors and Spectroscopies, and IPG Photonics Corporation consultant. His main fields of interest include tunable solid-state lasers, laser spectroscopy, and quantum electronics. In 2004, the Institute of Electrical Engineers in the United Kingdom has named him and his team recipients of the Snell Premium award for the input in optoelectronics and development of Cr^{2+} :ZnS mid-IR external cavity and microchip lasers. He is a Fellow of the Optical Society of America, a Member of the American Physics Society, and SPIE. He has authored or coauthored more than four hundred scientific publications in the field of quantum electronics, has published 1 book, several book chapters, and holds eighteen patents.

Vladimir V. Fedorov was born in Moscow, Russia. He received the M.S. degree in physical and quantum electronics from the Moscow Institute of Physics and Technology, Moscow, in 1985. He received the Ph.D. degree in physics for his work on color center lasers and laser spectroscopy of the Rare Earth aggregate centers in the fluoride crystals from General Physics Institute of the Russian Academy of Sciences, where he joined as a Research Fellow in 1987. His research interests include coherent and laser spectroscopy of doped solids, nonlinear optics, color center physics, and solid state lasers. Since 2000, he has been working at the Department of Physics of the University of Alabama at Birmingham (UAB), USA. He is currently a Research Assistant Professor, and Senior Scientist Consultant of IPG Photonics Corp. During recent years, his research has been focused on physics of laser media based on semiconductor materials with transition metals impurities. He is a Member of the Optical Society of America, and the International Society for Optical Engineering. He with colleagues received "Snell Premium" of the Institute of Electrical Engineers of the United Kingdom in 2004.

Dmitry Martyshkin was born in Barnaul, Russia, in 1973. He received the B.S. degree in physics from Novosibirsk State University, Novosibirsk, Russia, in 1996, the M.S. and Ph.D. degrees in physics from the University of Alabama at Birmingham, Birmingham, AL, USA, in 2000 and 2004, respectively. From 2003 to 2006, he was a Scientist at Altair Center LLC, USA, Massachusetts, from 2006 to 2010, he was a Research Associate at the University of Alabama at Birmingham, where since 2010, he has been Research Assistant Professor. He is author of more than 40 articles. His research interests include laser spectroscopy, laser biomedical applications, novel transitional metal doped ternary, and quaternary II–IV materials for laser applications.

Igor S. Moskalev was born in Belarus, in 1973. He received the Bachelor's degree in physics from Novosibirsk State University, Russia, in 1996 and till 1998 he worked as a Research Assistant in the Institute of Laser Physics, Novosibirsk, Russia, where he was involved in development of a highly stable, single frequency, diode pumped Nd:YAG laser with intracavity frequency doubling. Since 1998 till 1999, he worked as a Research Assistant in Hong Kong University of Science and Technology where he studied algal motility using a modified laser PIV system. He joined the Department of Physics of the University of Alabama at Birmingham (UAB), Birmingham, AL, USA in 2000 and received the M.S. degree in physics in 2002, and the Ph.D. degree in physics in 2004 from UAB for his work on development of ultrabroadband, multiwavelength, tunable semiconductor, and Cr^{2+}:ZnSe solid-state lasers. With colleagues, he received the "Snell Premium" of the Institute of Electrical Engineers of the United Kingdom in 2004 for development of Cr^{2+}:ZnS mid-IR external cavity and microchip lasers. He is currently working as a Senior Scientist at IPG Photonics Corporation, Middle-Infrared Lasers group and is involved in development of novel laser systems based on semiconductor materials with transition metals impurities.

Mike Mirov received the Bachelor's of Science degree in electrical engineering and the Master's of Science in engineering both from the University of Alabama at Birmingham (UAB), Birmingham, AL, USA, in 2006 and 2014, respectively. He was an Engineer at the Center for Biophysical Sciences and Engineering, UAB, from 2006–2010. Since then, he has been with IPG Photonics Mid-IR Lasers, where he is currently the General Manager. His research interests include laser materials, laser system engineering, and Mid-IR laser applications.

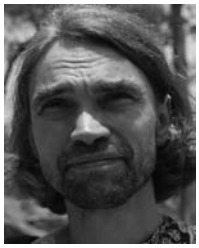

Sergey Vasilyev was born in Kisinau, Moldova, in 1972. He received the M.S. degree in physics from the Moscow State University, Moscow, Russia, in 1995 and the Ph.D. degree in physics from the General Physics Institute, Moscow, in 1998.

From 1998 to 2002, he was a Research Assistant with the Atomic Spectroscopy Laboratory, General Physics Institute. From 2002 to 2006, he was a Senior Research Assistant with the Laser Materials and Technology Research Center, Moscow. From 2002 to 2011, he was a Research fellow with the Institute for Experimental Physics, Düsseldorf, Germany. Since 2011, he has been a Laser Scientist with the IPG Photonics, mid-IR laser division, Birmingham, AL, USA. He is the author of more than 30 articles. His research interests include nonlinear optics, quantum optics, laser spectroscopy, laser research and applications.